Report for the Arbuckle-Simpson Hydrology Study:

Evaluation of Fracture Properties of the Arbuckle-Simpson Aquifer

OKLAHOMA STATE UNIVERSITY
Boone Pickens School of Geology
105 Noble Research Center
Stillwater, OK 74078-3031
405.744.6358, FAX 405.744.7841

Evaluation of Fracture Properties of the Arbuckle-Simpson Aquifer

FINAL REPORT

by:

Todd Halihan
Sassan Mouri
Jim Puckette

Oklahoma State University
Boone Pickens School of Geology
105 Noble Research Center
Stillwater, Oklahoma 74078

October 5, 2009
Stillwater, Oklahoma

Submitted to:

Oklahoma Water Resources Board
3800 North Classen Blvd.
Oklahoma City, OK 73118

Cover: Photograph of Sassan Mouri measuring fractures in the Blue River upstream of Connerville, OK

Table of Contents

Table of Contents (con't)

List of Figures

List of Figures (con't)

List of Figures (con't)

List of Figures (con't)

List of Figures (con't)

List of Figures (con't)

List of Tables

Acknowledgements

We would like to thank Dr. Carla Goad, OSU Statistics, for assisting with the statistical methods utilized in this report. We would also like to thank Jason Faith, Khayyun Rahi, and Michael Sample, OSU Geology, for their assistance in the field. Thanks also go to Dr. Brad Wolaver, Flinders University, South Australia who provided a thoughtful review of this report.

1.0 Executive Summary

As part of the Arbuckle Simpson Hydrology study, an evaluation of the aquifer's fractures characteristics was undertaken to evaluate the controls on the flow system. This evaluation examined a range of data types in order to evaluate fracture controls over horizontal and vertical flow in the aquifer. Understanding these controls allows more effective management models to be constructed, and assists in understanding what areas may contribute flow to springs and streams in the area.

GIS data for streams and faults were evaluated in the context of hydraulic and outcrop data in the aquifer. The results indicate that a dominant $170^{o} – 0^{o}$ trend evident in stream data exists over the study area as well as a less dominant $20 – 30^{o}$ trend that exists in both stream and fault data. The dominant fault orientation at 115^{o} does not provide a statistically significant signal in either fault or stream data. The stream density data indicate that no trends exist between density or length and stratigraphy, but geological processes appear to have a significant influence on stream orientations in the study area. The $170^{o} – 0^{o}$ trend appears to exert the largest control over surface water features, and appears to align with convergent flow patterns in most streams over the discharge region of the Hunton anticline. The exception is the Blue River which appears to be controlled by the location of the Simpson formation in the eastern portion of the Hunton anticline. The dominant fault orientation at 115° does appear to influence groundwater, at least in the northern portion of the Hunton anticline where it provide a linear connection between the orientation of the Blue River and the location of Byrds Mill Spring.

The evaluation of vertical fracturing included geophysical and thermal datasets. The temperature data indicate that the aquifer is well connected vertically with flow processes nearly eliminating any geothermal gradient in the aquifer. The geophysical methods applied to the aquifer include seismic, gravity, and electrical methods, and all observed significant vertical fracturing, which available data indicate extends to the bottom of the aquifer. The lower boundary of the aquifer is still poorly defined, but is likely to be 1000 meters or greater in some areas. The results indicate that pumping at depth in the aquifer will likely be directly connected to springs and streams.

2.0 Introduction

As part of the Arbuckle Simpson Hydrology study, an evaluation of the aquifer's fractures characteristics was undertaken to evaluate the potential controls on the flow system. As fractured rock aquifers present unique characterization challenges, the results of these evaluations can provide valuable evidence to understanding the hydraulic data collected in these aquifers.

2.1 Importance of Fracture Evaluation

The hydraulic characteristics of fractured rock have been difficult to study, due to the heterogeneous nature of fractured aquifers. Others have also studied fractured rock characteristics to determine hydraulic properties of the aquifer which include: Zimmerman and Bodvarsson (1996), Wanfang et al. (1997), Leveinen et al. (1998), Or and Tuller (2000). Fractures are known to modify both the flow velocity and direction and are critical to understanding flow at many scales.

Lineaments (i.e. linear features in data or images; often in aerial photos or outcrops) have been studied to delineate subsurface characteristics, which are known to correlate with surface patterns (Blanchet, 1957; Mollard, 1957; Rumsey, 1971; Parizek, 1975; Gleeson and Novakowski, 2008). Many fractures and faults are exposed at the surface creating lineaments (Mabee and Hardcastle, 1997). A number of different methods are employed to analyze lineaments and their effect on subsurface characteristics and influence on ground water flow. Lineaments have also been used in ground water research to determine where the best location would be for a competent well (Lattman and Parizek, 1964; Sander et al., 1997; Magowe, 1999; Moore et al., 2002). Lineament studies have also been used by the petroleum industry to improve well siting (Blanchet, 1957; Mollard, 1957, McQuillan, 1986; Evenson, 1989; Friesatz, 1991; Terech, 2005).

Many of the investigations conducted on lineaments have used aerial photographs (Sander et al., 1997; Magowe, 1999; Mabee et al., 2002; Moore et al., 2002). The use of LANDSAT and side-looking aerial radar has been the most common methods used. Various scales of the images are also used when trying to determine regional lineament characteristics.

Geographical Information Systems (GIS) has become widely used in the geological sciences. GIS coverages are easily available for most areas, or data layers can easily be created by digitizing maps. Aspect, hillslope, and degree slope change can be readily analyzed if a topographic map is available. GIS has become an important aid for mapping geology and rock properties in regions with subtle topography (Belt and Paxton, 2005).

Evidence has shown that a correlation can be made between surface lineaments and subsurface fractures. Lineaments that have a permeable overburden have been found to correspond to higher flows in wells (Mabee et al., 2002). Surface water near lineaments has also been found to produce higher flow (Mabee et al., 2002). Streams and faults are lineaments that have not been fully utilized to assess subsurface characteristics. Developing a quantitative understanding of aquifer characteristics can be a time consuming and costly task, however, stream beds can be recognized easily around the world and are perhaps the most unbiased and cost effective lineament type available to researchers. The use of GIS data sets allows for a significant increase in the amount of data that can be analyzed quantitatively. The methods introduced in this study should be applicable to studies of fractured aquifers in most geological settings.

2.2 Limits on Fracture Evaluation in the Arbuckle-Simpson

Every fractured aquifer presents challenges for determining the distribution and properties of the fractures controlling flow in the aquifer. The Arbuckle Simpson aquifer presents some unique challenges which are not common to many fractured aquifers. During the investigation several quarries were visited to determine if fractures were available for study in the quarry outcrops. The quarries presented few fractures, and the ones that were present appeared to be influenced by quarrying activities. Outcrops were examined on Delaware Creek and at Bird's Mill Spring without finding significant fracturing that could be used for evaluation. In addition, the extreme thickness (~1000 meters) of the aquifer limited a characterization of fracture properties with depth. This issue is combined with the anecdotal drilling evidence that the permeability of the aquifer appears to increase with depth. These factors led to attempting some common approaches in limited areas where data could be found with some new approaches that allowed a greater quantity of fracture data to be evaluated.

As a limited amount of transmissivity data exists for well tests, and outcrop fracture data is limited, many statistical approaches to fractured aquifers are unavailable. The structural complexity and extreme depth means that sets of data need to be combined to develop a conceptual model for the influence of fractures on the flow field that will be improved over time.

2.3 Objectives

The objectives of this study centered on determining the orientation and controls that fractures exert on the regional flow system in the horizontal plane, and evaluating the controls that fractures exert in the vertical plane. These two objectives were approached with different datasets. In the horizontal plane, surface data were collected from outcrops and GIS data were evaluated from fault and stream maps. These data were evaluated in the context of the potentiometric surface of the aquifer. In the vertical plane, geophysical data from seismic and electrical methods were combined with an analysis of a temperature log from the deep well installed for this study.

In the horizontal plane, the hypothesis that was tested for this study is that stream and fault characteristics (orientation, length, and density) will correlate to subsurface fracture characteristics which will help determine hydrogeological controls over the aquifer. In order to test this hypothesis, a method to analyze polymodal data from GIS layers was developed. Field data was collected to confirm interpretations from the GIS streams and faults layers. The data were evaluated in a geologic context using the structural history of the area and current stress fields. Two different GIS data grid sizes were used over the study area for a more detailed analysis of stream and fault characteristics and subsurface fracture patterns over different lithologies. The analysis of the combined data was used to make flow direction predictions from potentiometric data collected in the aquifer.

In the vertical plane, the hypothesis that was tested is that interpreted fracture patterns from various geophysical methods could be used to evaluate the context of temperature logs to determine if a consistent flow pattern could be interpreted from the various datasets.

3.0 Site Description

The Arbuckle-Simpson aquifer outcrops over an area of over ~500 mi^2 in southern Oklahoma. It lies beneath the Murray, Carter, Johnston, Pontotoc, and a small portion of western Coal County (Figure 1). The Arbuckle-Simpson aquifer includes formations from the Arbuckle Group (Upper Cambrian to Lower Ordovician) and the Simpson Group (Middle Ordovician). The aquifer is composed of mostly limestone, dolomite, and sandstone. The formations have been folded and faulted due to major uplifts in the area during Early to Late Pennsylvanian time (Fairchild et al., 1990). Secondary porosity is created by fractures, joints, and solution channels (Fairchild et al., 1979). Many of the springs in the area supply the perennial streams (Fairchild et al., 1990).

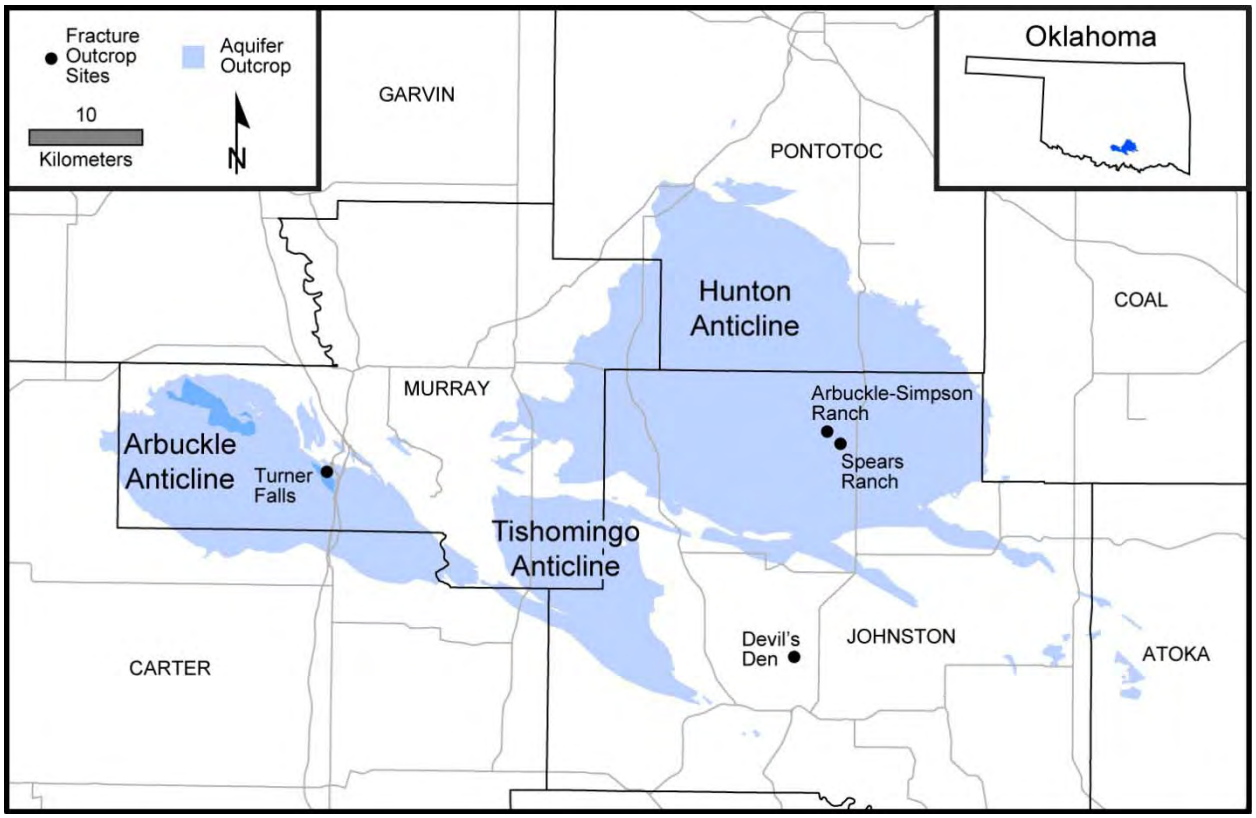

Figure 1. This regional map shows the location of the outcrop area of the Arbuckle-Simpson aquifer and outcrop fracture mapping sites. Major roads are in light gray; county boundaries are in black.

The structural history of the region is one that has been extensively studied (Decker and Merritt, 1931; Dott, 1933; Dott, 1934; Ham, 1955, Ham et al., 1964; Johnson, 1991a; Johnson, 1991b). The Arbuckle-Simpson Mountains are part of the southern Oklahoma Aulacogen (Wickham, 1978). A brief description of southern Oklahoma's structural history can be broken into three stages based on Wickham (1978). First, the rifting state occurred, which was a period of uplift. Both intrusive and extrusive activity was present. Sedimentation was of a continental scale during this time. During the second state subsidence occurred. A formation of a passive continental margin, marine transgression, and rapid subsidence occurred. Thick sedimentary sequences were being formed. The final stage was the deformation stage. Reactivation of old fault trends occurred with strike slip and dip slip displacements being the dominant fault activity. Local basins and uplifts were formed during this time. Due to the activity of the region, conglomerates were also formed during this time.

Some dominant fault trends can be seen as a result of this failed rift zone. During the Paleozoic, an inversion of the rift began during the Late Mississippian to early Permian. During this process a belt of west to northwest trending uplifts and faults were created (Marshak et al., 2003). Inversion of the alaucogen shortened orientations perpendicular to the rift axis in an east to southeast direction (Marshak et al., 2003). Many faults during the alaucogen began to change. Normal faults became reverse faults, and during times of compression folds began to form. Left and right lateral, strike-slip faults, normal faults, and reverse faults characterize the area, as well as some flower structures (Marshak et al., 2003). In the Tishimingo-Belton anticline, lineament orientations were found to be dominantly $N50^{o} – 60^{o}W$ (Denison, 1995).

4.0 Horizontal Fracture Evaluation

Understanding horizontal fracture properties can provide an understanding of preferred flow directions and well capture zones in a fractured rock aquifer. In evaluating fracture control over horizontal flows in the Arbuckle-Simpson, fracture data from outcrops were collected along with the evaluation of GIS datasets of faults and streams. New methods were developed for evaluating orientation and the data were used to evaluate the effect of the dominant fractures in the context of the available hydraulic data. Additional details are available in Mouri (2006).

For the horizontal orientation, stream and fault orientations are evaluated to better analyze the data. Calculations for the density of streams and faults have also been used to characterize the study area. Field data collection is also compared to the GIS streams and faults layer. A table is created to better visualize the relationships. The results of the statistical analysis of orientation and length are presented to better understand preferred orientations. The analysis will help better characterize strong and weak orientations for streams and faults in the study area. Field work and stream data correlation is also discussed in this section. Finally, the effects of preferred orientations on the horizontal flow field are evaluated.

4.1 Methods

The methods used range from large to small scale across the aquifer. The GIS and field data focus on characterizing faults and streams as lineaments in the aquifer. The methods used to extract stream and fault data from GIS databases are described followed by collection of field data at four field sites. The methods used to analyze these data are described for the statistics and power law relationships derived for the data. Finally, the methods used to compare the various datasets are described.

Hydraulic data is evaluated to determine fracture controls by first describing the methods of calculating hypothetical anisotropic flow nets for the aquifer, given assumed fracture control orientations. Additionally, fracture connections between surface and groundwater are explored using methods described in section 4.1.7.

4.1.1 GIS Data Extraction

GIS stream and fault layers were converted to line segments to study length, orientation, and density of fractures or fracture proxies. The GIS layers used were obtained from the Oklahoma Water Resources Board who compiled the layers as part of the Arbuckle Simpson Hydrology Study. The stream and fault layers were sent to the Department of Primary Industries and Resources in South Australia to be processed into point data. They created the nodes in GIS with ArcInfo Workstation and used the commands SHAPEARC and UNGENERATE to acquire Northings and Eastings of beginning and ending nodes of each line segment in the x (easting) and y (northing) direction in the data layers. The study area was overlaid by 77 10-km grid cells (Figure 2). A set of higher resolution grids was created to help determine the relationship between stream characteristics and lithofacies. The higher resolution grid contained 304 2.5-km grid cells. The size of the grid cells was determined by the data density of stream and fault data in the area. In the x-direction (easting) the study was approximately 11,000 meters long and in the y-direction (northing) the length was approximately 7,000 meters. Each 10-km grid cell contains between 260 to 1500 stream segments and 0 to 100 fault segments.

To determine the length and orientation of the GIS segments, a point halfway between the endpoints of a line segment was called a midpoint (Figure 3). Midpoints of each stream segment were obtained to determine the cell position of each stream segment. This allowed for an analysis of each grid and eliminates segments crossing multiple grid cells. Midpoints were found using basic algebra (Equation 1).

$$(x_m, y_m) = \left(\frac{x_1 + x_2}{2}, \frac{y_1 + y_2}{2} \right). \quad (1)$$

The lengths of each line segment were found by using equation 2 (Figure 4).

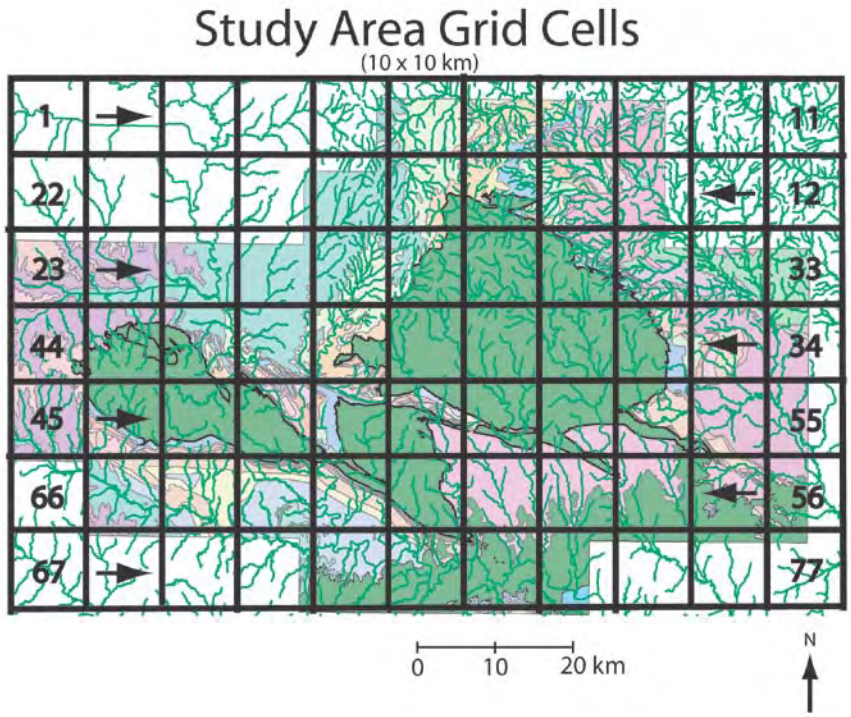

Figure 2. The Arbuckle-Simpson study area over laid by 10 km grid cells. Each grid cell has a 100 km^2 area.

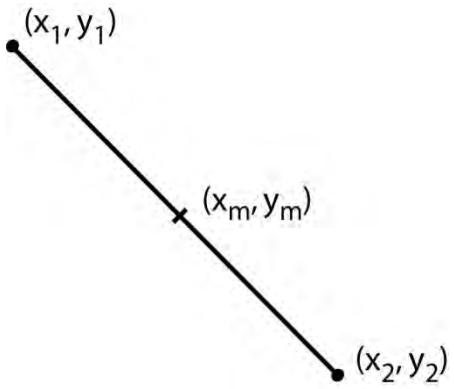

Figure 3. This figure illustrates where the midpoint was located on a line between two data points.

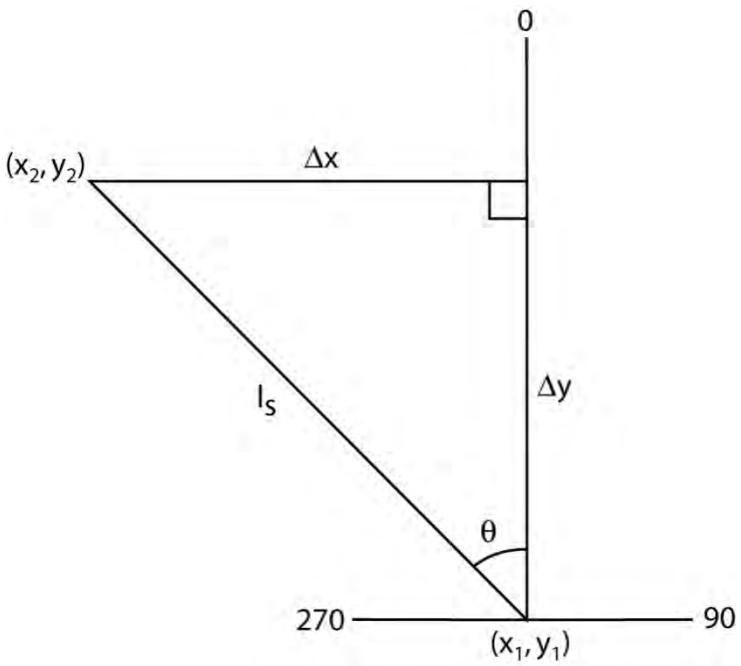

Figure 4. Geometry defining the distance and angles used to find lengths and orientations of streams and faults.

The formula to find lengths was known as the distance equation (Equation 2),

$$l_s = \sqrt{(x_2 - x_1)^2 + (y_2 - y_1)^2} \quad . \tag{2}$$

By rearranging the formula, orientation was found using:

$$\theta_s = \sin^{-1}\left(\frac{x_2 - x_1}{l_s}\right). \tag{3}$$

Since the orientations were analyzed between 0^o – 180^o, negative values were corrected using:

$$\theta = \theta_s + 180\,. \tag{4}$$

The density of each grid cell was analyzed by obtaining the total length of the streams in the grid and dividing that number by the area of the grid. A density map was only created for the 10-km grid cells, which equals a total area of 100 km^2 for each grid cell. A smaller grid was constructed over the study area to acquire a better resolution of trends over the Arbuckle-

Simpson aquifer. It enables a better analysis of stream characteristics in different lithologies. The smaller grid that was created contained cells that were 2.5 kilometer on each side. Each 2.5-km grid cell contained approximately 100 streams.

The smaller grids allowed for a detailed view of orientation trends to give a better resolution and help strengthen the correlation between the lineaments and subsurface characteristics. The 10-km grid resolution combined with the 2.5-km resolution strengthened observations by providing a better view of which lithologies were affecting each grid cell. This data, combined with field work and potentiometric maps over the area allowed for aquifer characteristics to be better understood. The trends observed in the small grids indicated which lithologies are creating certain behaviors in stream characteristics.

A shaded relief, hillslope map, and an aspect map for the study area were used as visual aids to determine if the direction of the slope is affecting the orientations observed in the streams and faults GIS layers. A general lithology map was also created to help better understand stream and fault characteristics in different lithologies.

4.1.2 Field Data Collection

Field work was conducted at four different locations where exposed bedrock with fractures was present (Figure 1). The locations were chosen based on availability of bedrock exposure over the Arbuckle Mountains. Locations that were near streams were preferable. However, there are limited outcrops over the study area. The four locations were: Site 1 in Connerville, Oklahoma at the Arbuckle-Simpson Ranch (north of Blue River), Site 2 in Connerville, Oklahoma at the Spears Ranch (south of Blue River), Site 3 in Devil's Den, and Site 4 at Turner Falls, near Davis, Oklahoma (Figure 1).

Field work was conducted in the study area to correlate fracture characteristics seen in the field to stream characteristics. Exposed bedrock along streams enabled a scan line to be created perpendicular to prominent fracture orientations (Figure 5).

Figure 5. A scan line taken across fractures was used to gather data. One dominant trend is seen perpendicular to the scan line. A second fracture set can be seen parallel to the tape and has grass growing in one of the fractures in the set.

Location, length, and orientation of each fracture that crosses the scan line were determined. Length was measured using a 12-inch ruler for small fracture lengths. A measuring tape was used if the fracture length was longer than 12 inches. Orientation was observed using a Brunton azimuthal compass. A magnifying glass was used to increase fracture visibility and determine if the fracture was open or closed. If the fracture was closed, the fill material was analyzed to make a field determination of the composition of the fill.

4.1.3 Statistical Analysis of Orientation

Along with standard rose diagram analysis, an unbiased statistical polymodal orientation method to analyze stream and fault data was developed for this work to determine preferred orientations (Mouri, 2006). Circular statistics were not sufficient in correctly determining dominant orientations; which lead to the development of a new statistically appropriate method. The lack of confidence in existing circular statistics was due to the fact that they do not account for length-weighted data and polymodal data. A stream segment that is long in length in a particular orientation must be considered a stronger signal. Figure 6 is an example of this scenario.

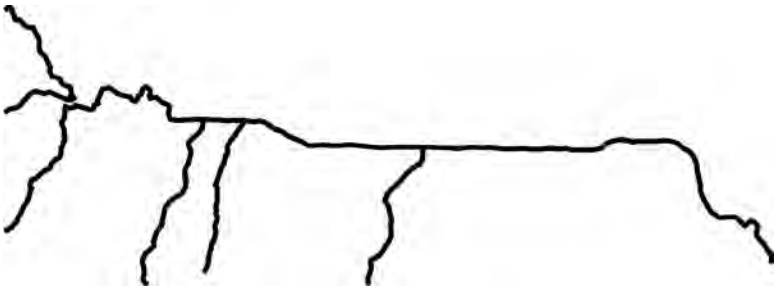

Figure 6. This stream segment has a preferred orientation towards the east-west, but traditional statistical methods would determine the north-south orientation was dominant.

To statistically analyze this stream reach, each orientation (θ) of the segment is weighted by the length (L) of a segment,

$$\theta_L = L_i \times \theta_i \ . \tag{5}$$

All the length-weighed orientations (θ_L) are summed in 10 degree bins. The sum of the θ_L is then divided by the total length in that orientation (L_T),

$$\theta_\varphi = \frac{\sum L_i \theta_i}{L_T} = \frac{\sum \theta_L}{L_T}. \quad (6)$$

By determining the mean and standard deviation of lengths in a grid cell, strong and weak orientations were identified using Equation 6. If θ_φ was one standard deviation above the mean of all eighteen θ_φ values, it was considered a weak signal; two standard deviations above the mean were considered strong signals. There were more than one strong signal in some grid cells. Strong signals indicated a preferred orientation of streams and faults in a particular grid cell. Weaker signals indicated that other orientations are present in the grid cell but may not be geologically significant.

To determine which orientations were preferred for the streams and faults GIS layer on a regional basis, histograms of the grid signals were created for the each datasets. A histogram of the sum of strong and weak signals for the binned orientations was observed for the 10 km and 2.5 km grids. The mean and standard deviation of the sums is used to delineate preferred regional orientations for each GIS layer. The GIS faults layer was the layer used to determine if a correlation can be made between orientation signals and fractures in the subsurface. The GIS faults layer should limit stream data biases because the faults are digitized off of a fault map. Again in this case, two standard deviations above from the mean indicated a preferred orientation.

4.1.4 Power Law Statistics for Length

The power law between two scalar quantities can be written as

$$\alpha = r s^t. \quad (7)$$

The variable α was the rank of the length of the stream, with α=1 corresponding to the longest fracture. The two variables r (constant of proportionality) and t (the exponent of the power law) were determined from the slope of a line using Excel.

When Equation 7 was rearranged to solve for *s*, the predicted length of the longest fracture was determined. By allowing α to equal 1, the longest fracture length was found by carrying out these steps,

$$1 = rs^t, \tag{8}$$

divide by *r*,

$$\frac{1}{r} = s^t. \tag{9}$$

To solve for *s* we must take the log of both sides

$$\log\frac{1}{r} = t\log s, \tag{10}$$

and taking the exponent of both sides rearranges the equation to

$$10^{\log\frac{1}{r}} = 10^{t\log s}. \tag{11}$$

By solving for *s* the length can be determined

$$s = 10^{\frac{1}{r}}. \tag{12}$$

The power law was used only to model stream lengths above 100 meters. The resolution from the GIS stream layer does not allow a precise determination of actual stream lengths below 100 meters. Previous work conducted on fractures supports this method (Cladouhos and Marrett, 1996; Marrett, 1996; Marrett et al., 1999; Ortega et al., 2006). They found that there is a minimum measurable length for fractures. Below a certain length, fracture lengths cannot be correctly measured and errors will be introduced into the data set.

4.1.5 GIS and Outcrop Data Comparison

One factor that is taken into consideration in this project was the affect geomorphology had on the stream orientations. A shaded relief map was used to study the influence hillslope had on stream density and orientation. An aspect map was also created to determine if the direction the slope was facing had an influence on the direction that the streams were oriented in a particular grid cell. The characteristics of stream density over the study area were observed by creating a map in GIS of the degree of slope change for the study area. By combining all of these maps and correlating them to the preferred orientations for the study area, an unbiased analysis of stream lengths, orientations, and densities was conducted.

The stream data contain two potential sources of bias. First, the digitizing of the layer may include more streams by one algorithm or person doing hand digitizing. Second, at lower resolutions, a pixilation bias may results in extra north-south or east-west segments. These were examined in the datasets by separating areas with higher apparent stream density if they appeared to be induced during digitizing. In orientation data, pixilation bias could be observed by extra signal strength at 0° or 90°. This bias is not expected in the fault dataset.

4.1.6 Anisotropic Flow Net Analysis

Once potential preferred flow directions are available from the outcrop and GIS data analysis, anisotropic flow nets were constructed to evaluate the influence of these potential orientations on flow direction. As regional scale estimates of the magnitude of anisotropy are difficult to obtain, the evaluation was performed with an anisotropy factor of three, which would correspond to the preferred orientation having a hydraulic conductivity that was nine times higher than the other directions. This would illustrate areas of the flow field that would have the greatest influence due to any anisotropic effects in the flow field.

This study used the USGS 1995 Synoptic survey for the Hunton Anticline as the primary dataset. Three points that left depressions in the surface were removed leaving 148 points in the dataset. The data were rotated to the appropriate orientation using the center of the domain as the rotational axis and then transformed to isotropic space and contoured in Surfer. The flow lines were then drawn by hand and the domain was returned to the proper spatial coordinates (Figure 7). This was done for orientations with significant fracture orientations.

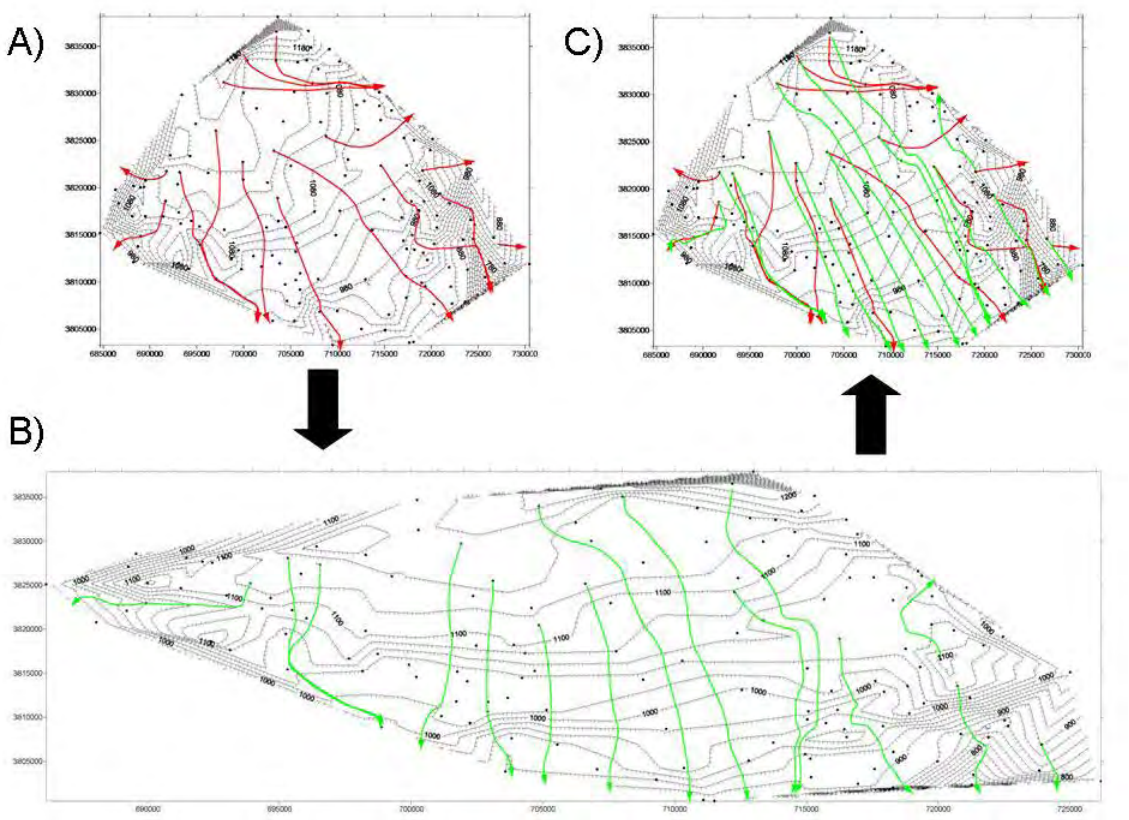

Figure 7. Anisotropic flow net methods. A) Water table data contoured with flow lines drawn assuming isotropic conditions. B) Domain altered to reflect anisotropy with a direction of 0 degrees (N-S), and an anisotropy factor of three with flow lines drawn. C) Comparison between isotropic and anisotropic flow lines.

4.1.7 Hydraulic Data

Data from two sources were used to augment the fracture analysis for horizontal controls on flow. USGS discharge data were collected at Byrds Mill Spring (USGS Gauge 07334200) and on the Blue River at Connerville (USGS Gauge 07332390) (Figure 8). The site at Connerville also had conductivity and temperature data available. The period of record used for this study was October 16, 2003 to December 3, 2007. The second source was data collected at the Spears Ranch in both the Spears 1 and Spears 2 wells and on the Blue River (Rahi and Halihan, 2009). The period of record used for this study was March 20, 2007 to February 29, 2008. The site on the Blue River was a temporary location downstream of the check dam on the Spears Ranch.

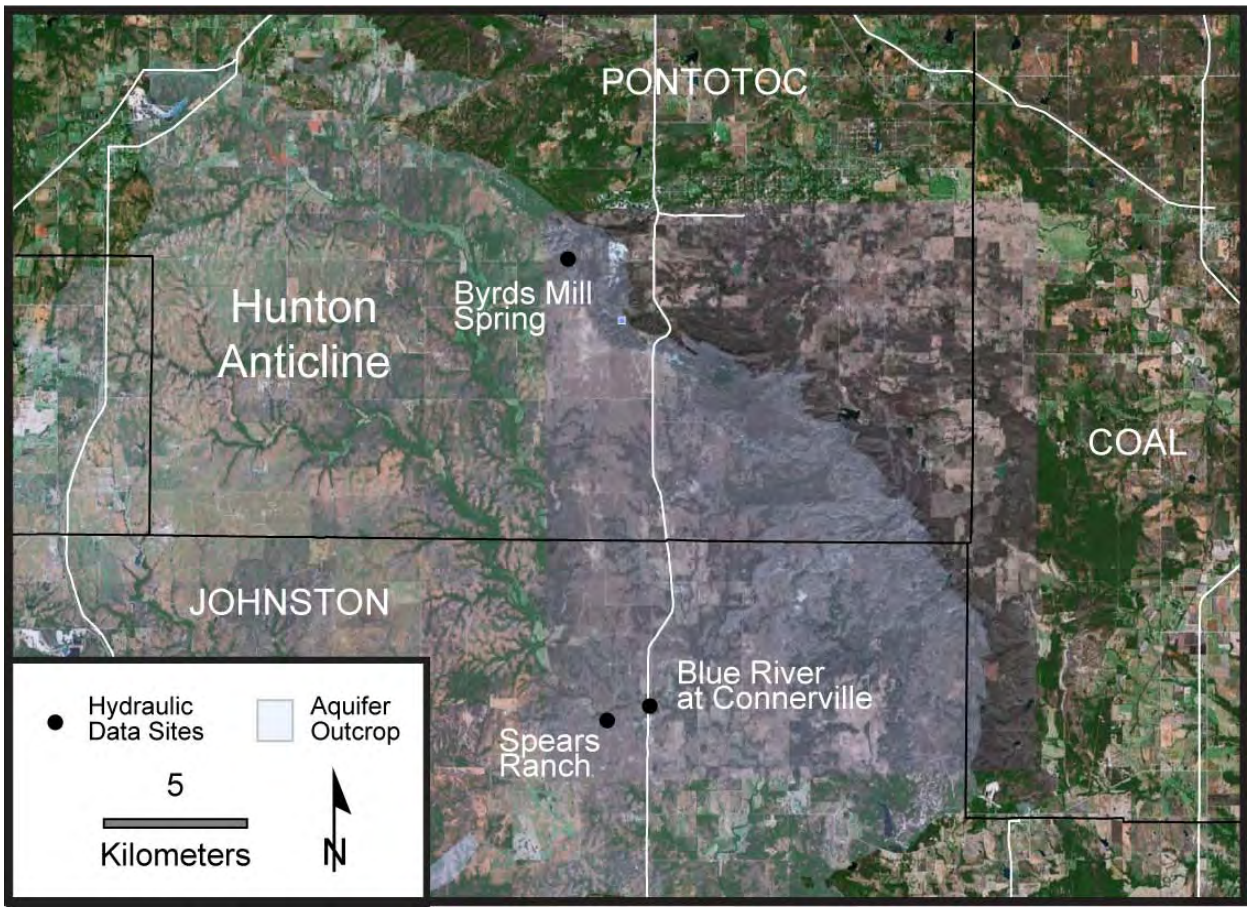

Figure 8. Site map for hydraulic data used in study. Major roads are white, and county boundaries are black.

4.2 Results

The results for the horizontal fracture evaluation used the range of data from large to small scale across the aquifer. The GIS data is analyzed and compared to the geomorphology of the area. Next, the results of the GIS and field data characterizing faults and streams as lineaments show the preferred orientations in the data. The statistics and power law relationships derived for the data are presented. Finally, the correlations between the various datasets are described.

The results of the hypothetical anisotropic flow nets for the aquifer, given assumed fracture control orientations, are presented. Finally, horizontal fracture connections observed in data between surface and groundwater are demonstrated.

4.2.1 GIS Data Analysis

The power law was used only for stream lengths above 100 meters (Figure 9). The resolution from the GIS stream layer does not allow a precise determination of actual stream lengths below 100 meters. By using only streams above 100 meters, the power law best predicts stream lengths. Previous work conducted on fractures supports this method (Cladouhos and Marrett, 1996; Marrett, 1996; Marrett et al., 1999; Ortega et al., 2006). They found that there is a minimum measurable length for fractures. Below a certain length, fracture lengths cannot be correctly measured and errors will be introduced into the data set.

Length trends for each formation can also be analyzed for the 2.5-km grid cells. Figure 10 shows the formation vs. length without the greater density bias removed. Figure 11 is a modified version with the greater density area removed.

The results from the GIS streams layer allowed for orientations to be plotted on rose diagrams. The rose diagram created for grid cell 40 is an example of one of many created over the study area (Figure 12). The scale created for the rose diagrams was determined by the maximum stream length in any orientation in the GIS stream data set. Grid Cell 31 had a maximum length of 17,078 meters and controlled the scale created. A complete map of all the rose diagrams over the study area is shown in Figure 13.

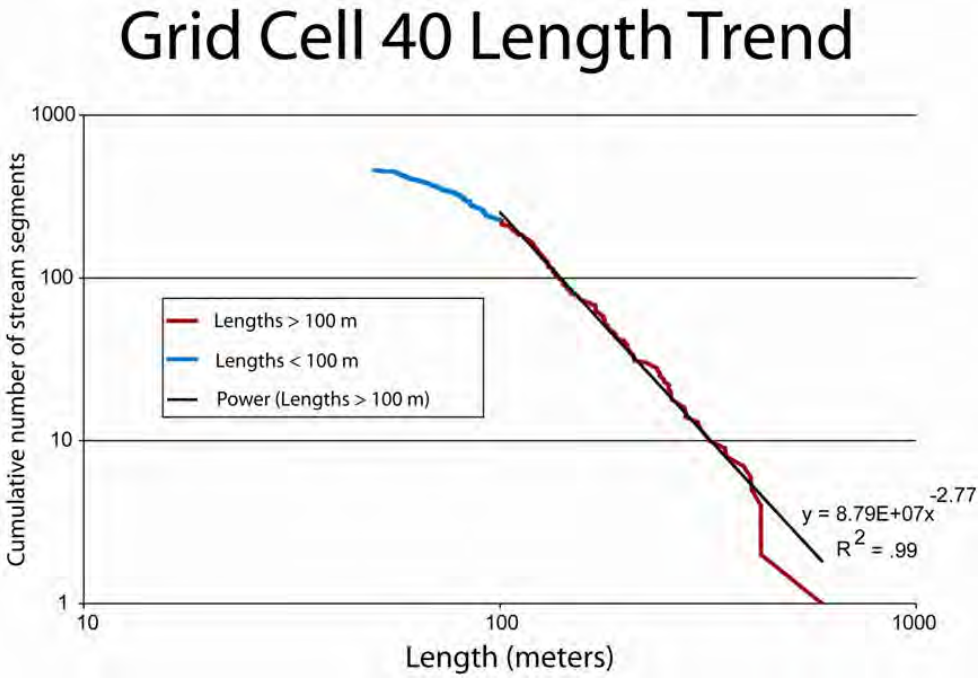

Figure 9. The stream length trend of grid cell 40 shows the power has a goodness of fit of 99% for length data greater than 100 m.

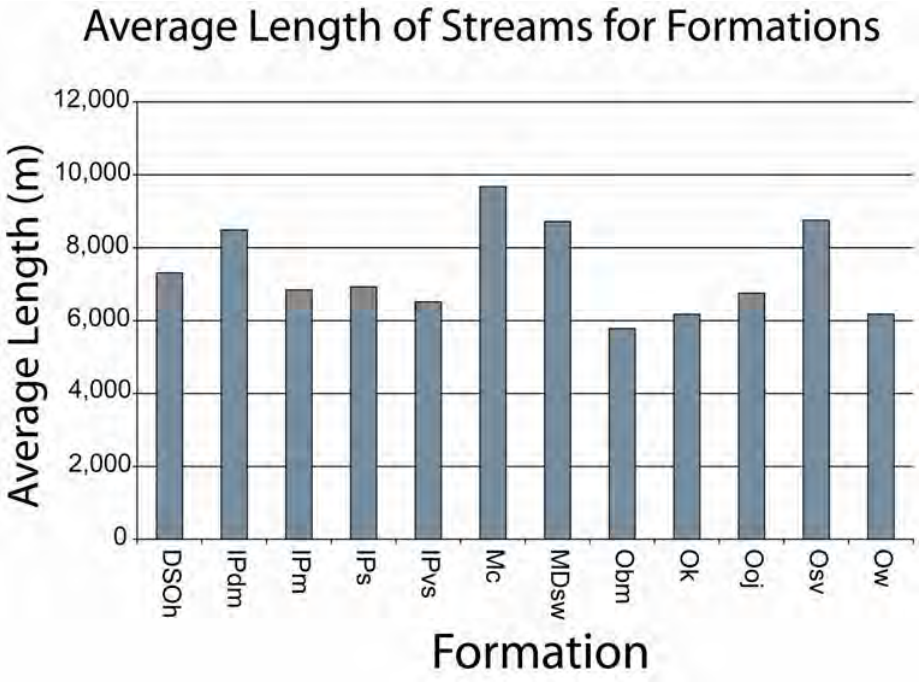

Figure 10. The average length of each formation for the 2.5-km grid cells is plotted as a bar graph to better visualize formation characteristics.

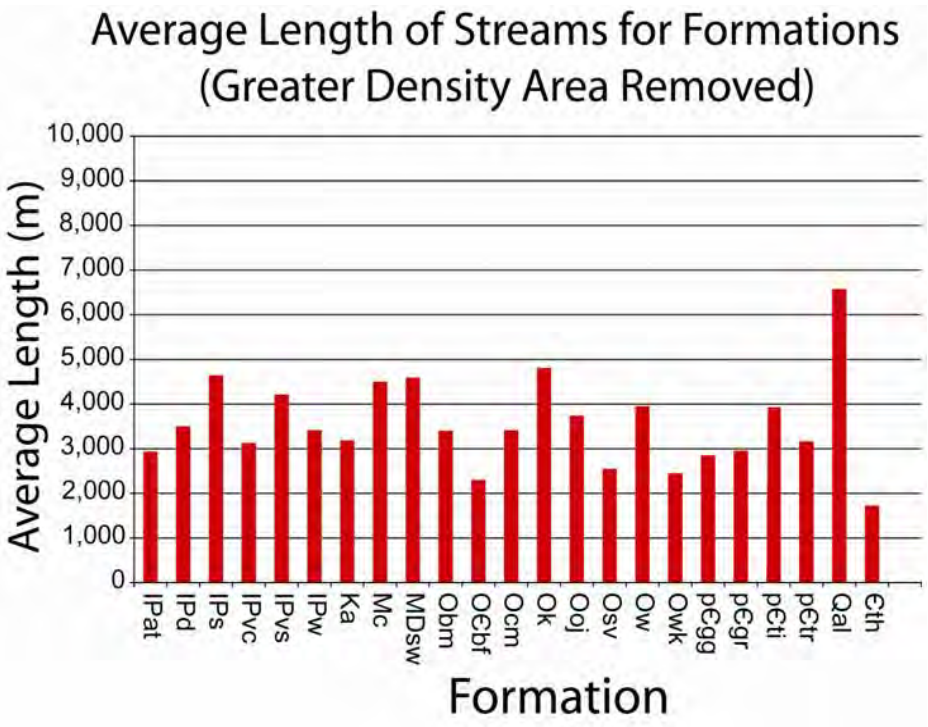

Figure 11. After the greater density area is removed the characteristics of each formation can be better analyzed.

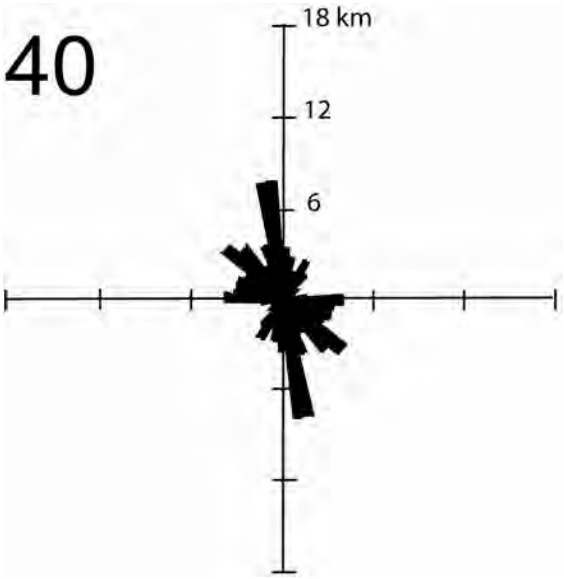

Figure 12. Rose diagram for streams in grid cell 40.

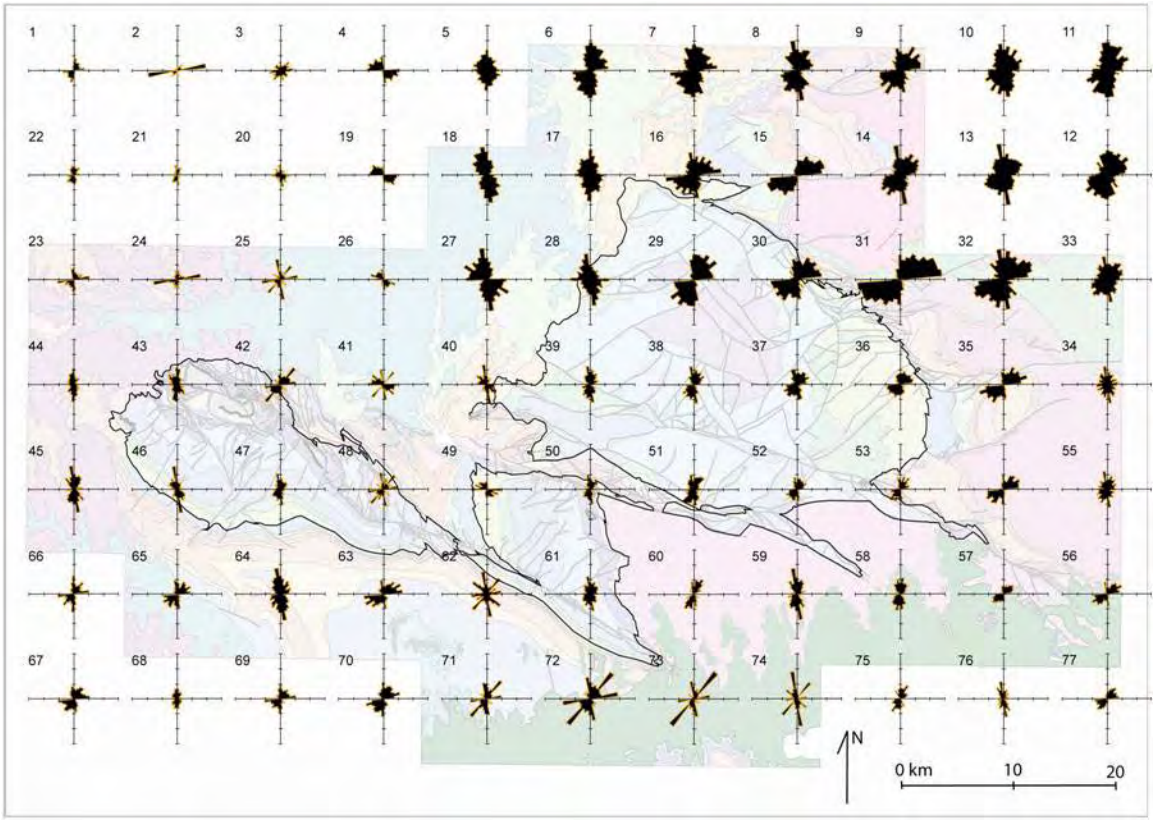

Figure 13. The 10-km grid cells with rose diagrams for each grid cell allow a visual aid to analyze stream orientations over the study area.

The 2.5-km rose diagrams were created for data over the Hunton Anticline. Figure 14 is an overlay of the rose diagrams onto the study area. It is difficult to determine trends using this figure, the statistical analysis of the 2.5-km rose diagrams will provide another visual aid to help delineate preferred orientations.

The density map (Figure 15) which was created will indicate what portions of the study area contain more streams. The top right portion of the study area contains a greater density of streams, which will be discussed in more detail later.

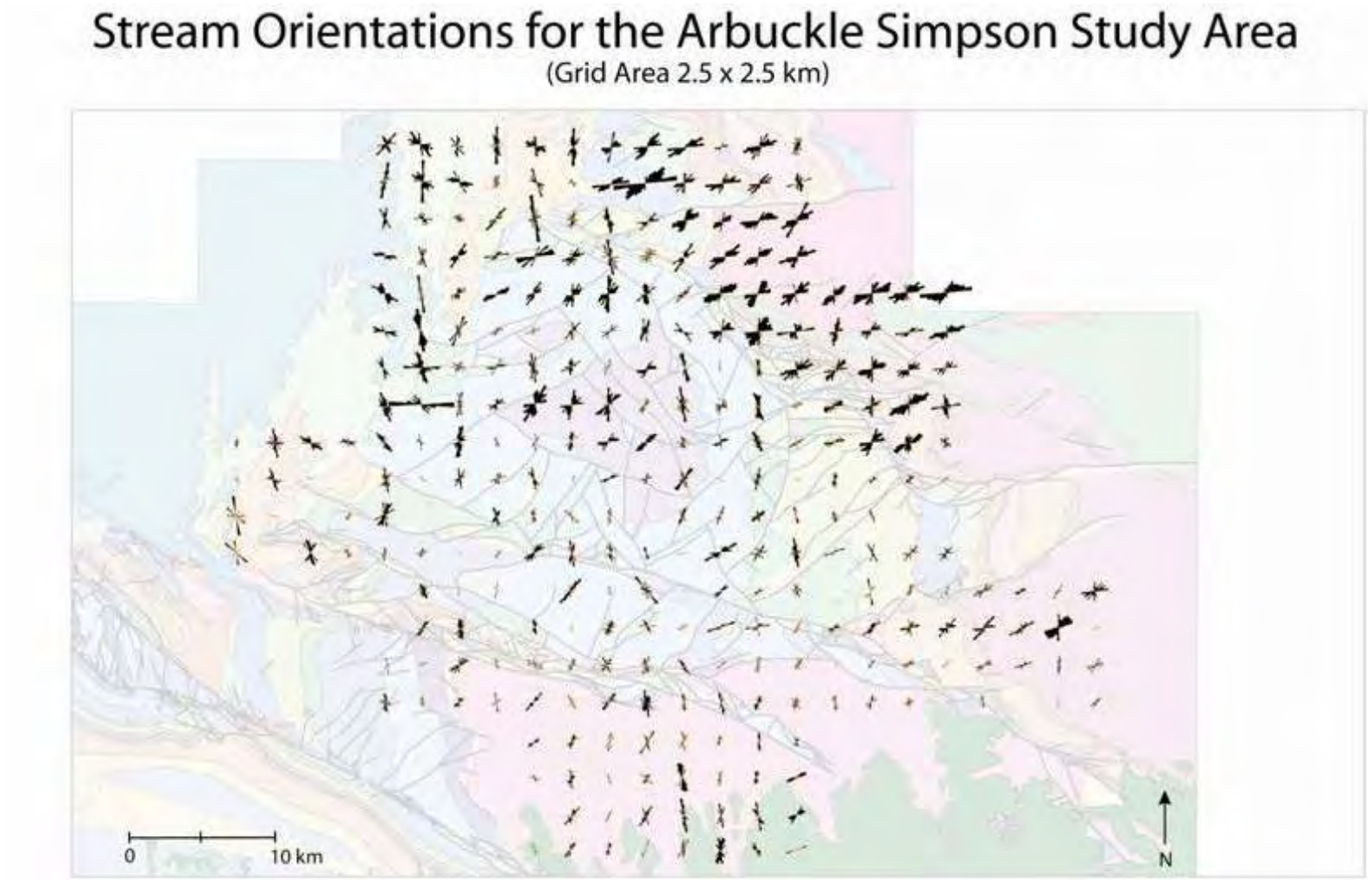

Figure 14. Rose diagrams for streams were created for 2.5 x 2.5 km grid cells for a more detailed interpretation over the Hunton Anticline.

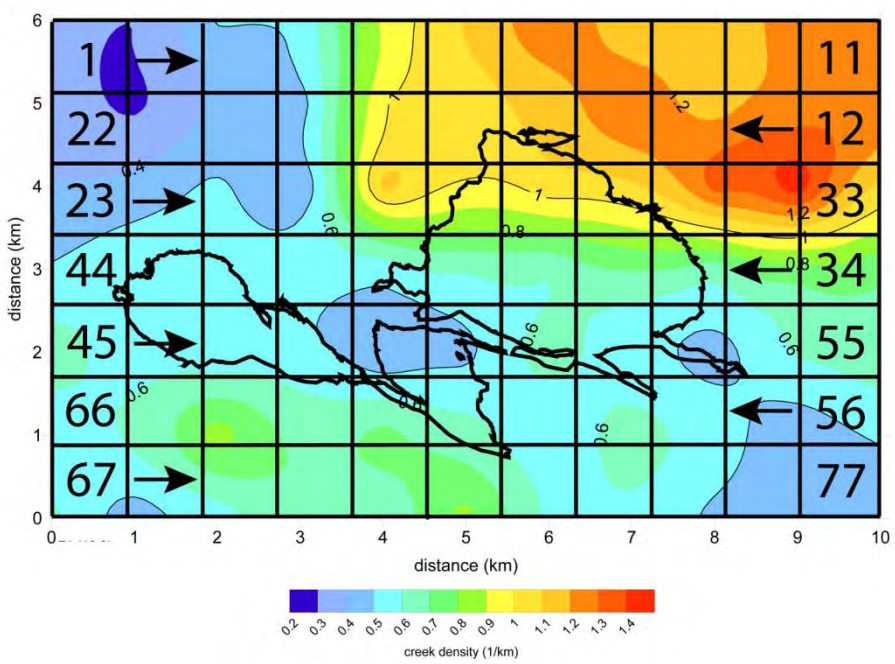

Figure 15. The density map over the study area indicates that there is a greater density of streams near grid cells 13 and 32 (second column from right). This is due to bias in the GIS stream created by human factors.

To fully understand the characteristics of different formations their densities were plotted on a bar graph (Figures 16 and 17). Due to the bias in GIS layer of stream density two different graphs are created. Figure 16 shows the density of streams for formations before the greater density area was removed from the data. Figure 17 shows densities after the greater density area is removed from the data.

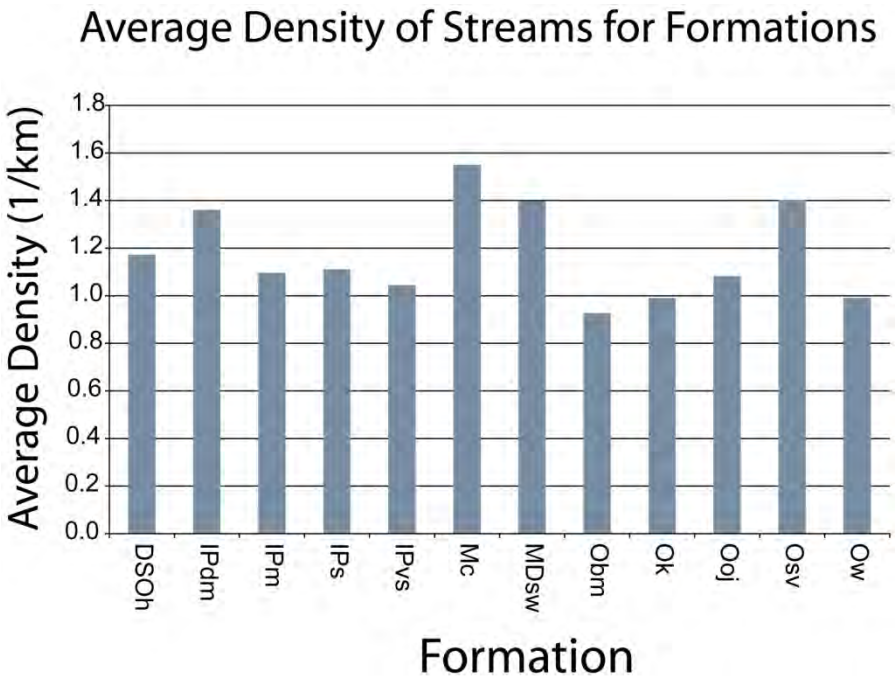

Figure 16. This bar graph shows that average density for each formation varies. The Caney Shale (Mc) has the greatest density of streams, but not a significant difference.

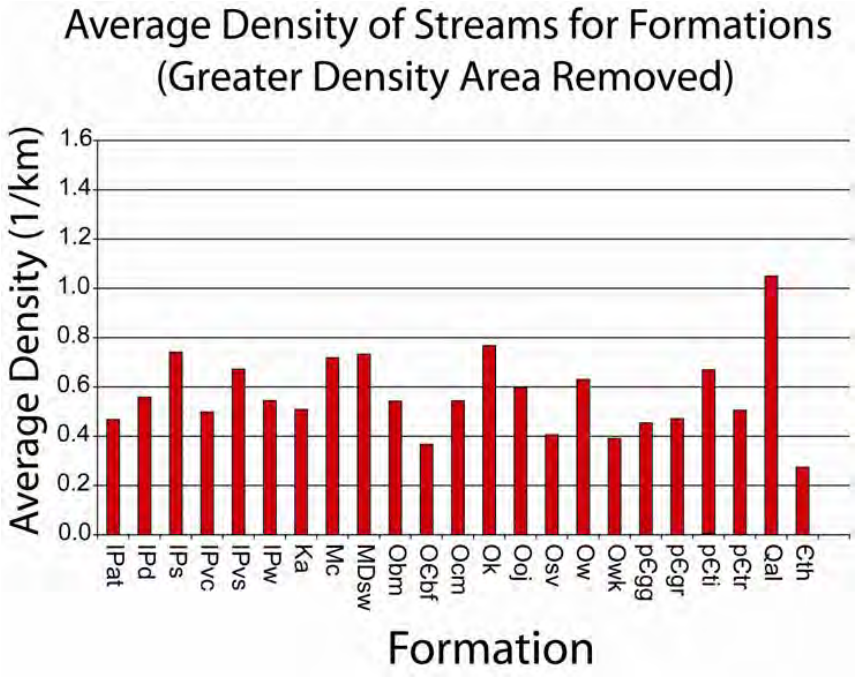

Figure 17. In this graph the Timbered Hills Group (Cth) has a low density of streams.

4.2.2 Geomorphology and Stream Orientations

The shaded relief map for the Arbuckle-Simpson Mountains indicated very little slope change over the Hunton Anticline (Figure 18). The aquifer area is outlined by a faint yellow line to better visualize the boundary. To make a complete analysis of the influence geomorphology may have on stream orientations it is necessary to create an aspect map for the study area (Figure 19) and a hillslope map (Figure 20). The maps were created using basic ArcGIS functions.

It is also necessary to analyze the general lithology of the study to better understand what the stream orientations may indicate. A more general map is created to determine if lithology may explain differences in stream orientations (Figure 21).

The lithology of the aquifer is mostly massive limestone and dolomites. It is difficult to find fractures outcropping on the surface as determined by many attempts to conduct field work in the area.

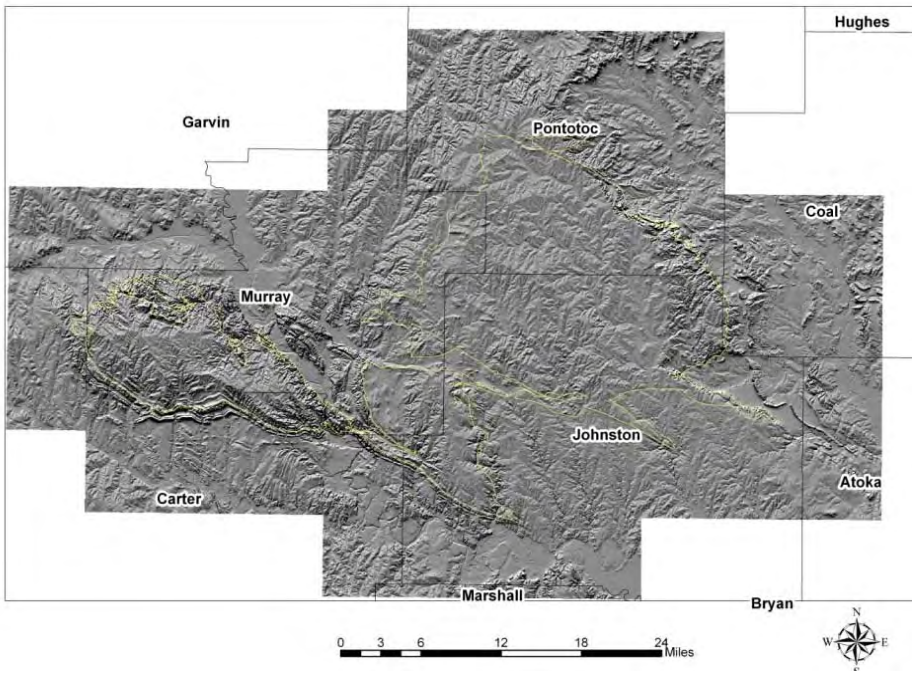

Figure 18. The shaded relief map for the Arbuckle-Simpson Mountains shows very little change in slope over the Hunton Anticline.

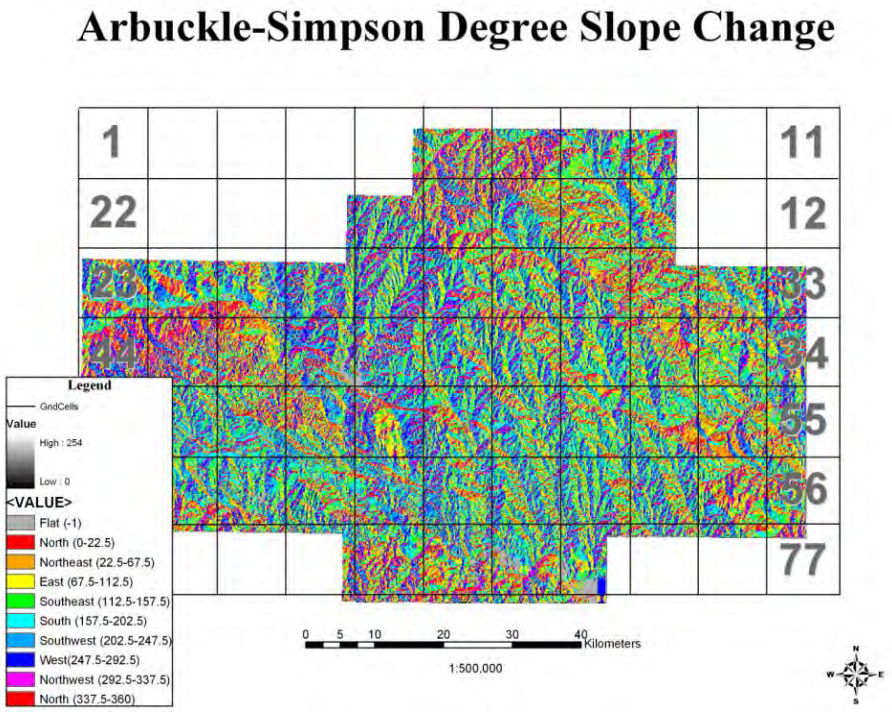

Figure 19. The aspect map for the Arbuckle-Simpson Mountains does not show a strong preferred hillslope direction.

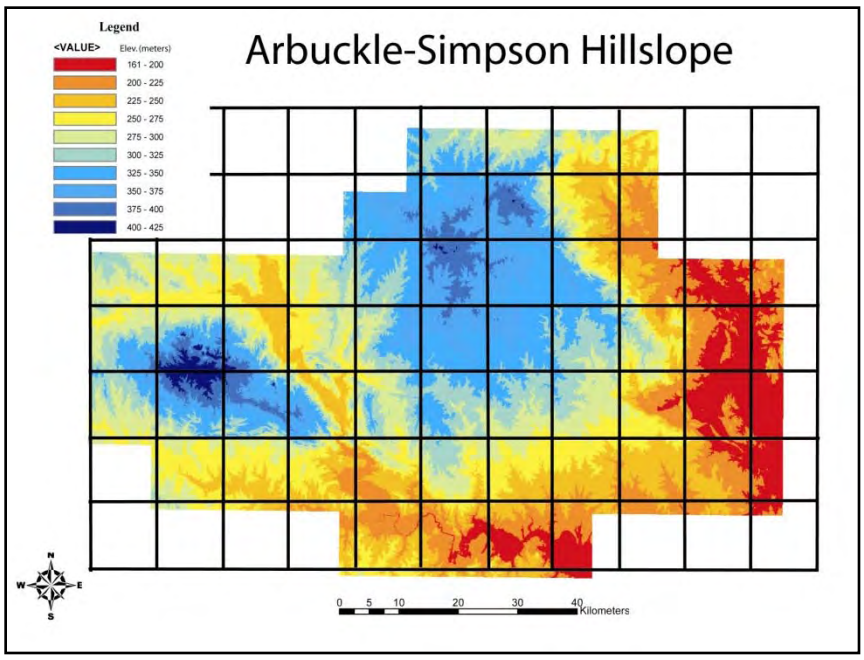

Figure 20. The hillslope map for the Arbuckle-Simpson shows very little change in elevation over the Arbuckle-Simpson Mountains.

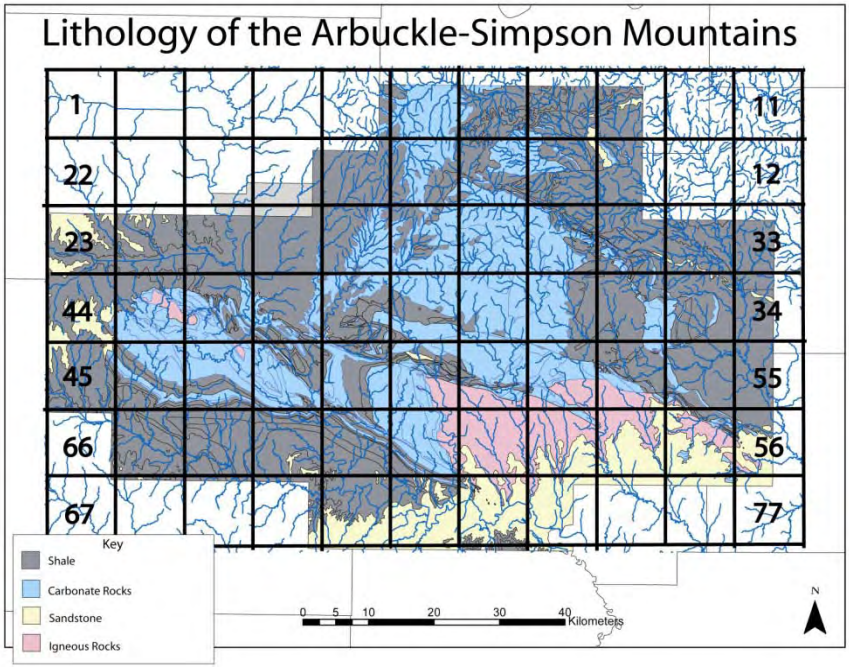

Figure 21. A general lithology map over the Arbuckle-Simpson Mountains indicates a mostly carbonate aquifer with surrounding shales and granites.

4.2.3 Orientation Analysis

By using the mean and standard deviation of the orientations for each grid cell it was possible to determine preferred orientations. Figure 22 indicates that each grid cell is unique and is better characterized by using this method. The preferred orientations predicted by this method vary in strength for all three grid cells.

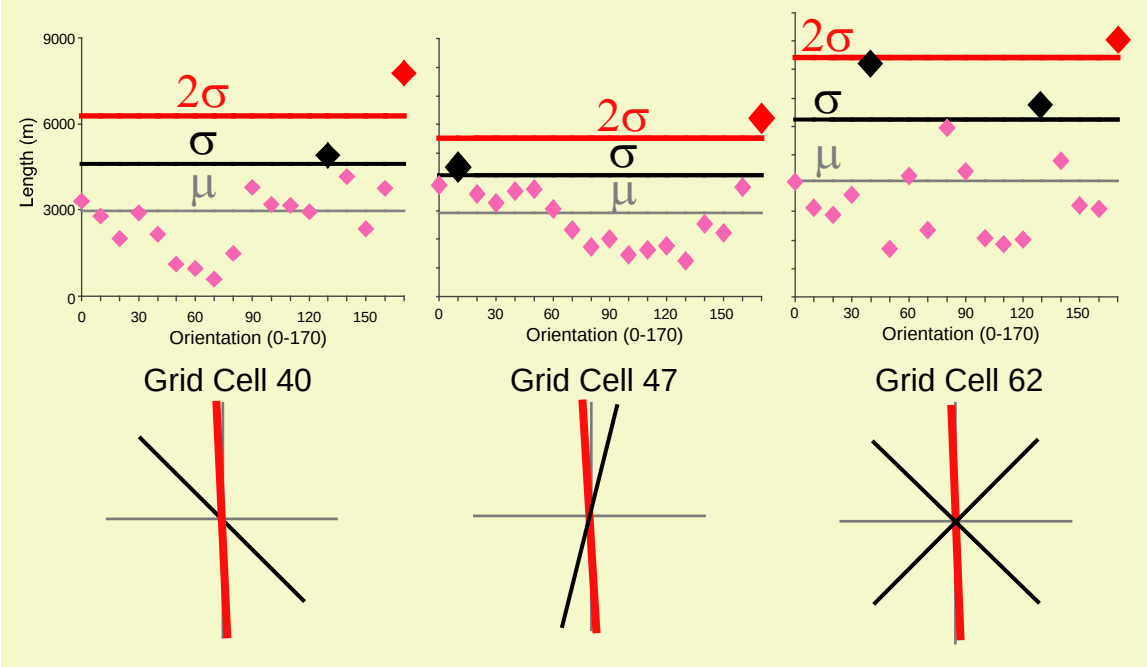

Figure 22. This figure shows that the statistics used to define preferred orientations allows for a better understanding of grid cell characteristics. The strength in the method is that is allows each grid cell to uniquely define preferred orientations. Grid cell numbers 40, 47, and 62 are shown in Figure 21.

4.2.3.1 Unimodal

Unimodal orientations indicate the streams are dominantly oriented in one direction (Figure 23). After statistically analyzing the data, it is evident that grid cell 2 is unimodal. Only one dominant orientation is present and no weak signals are present (Figure 23).

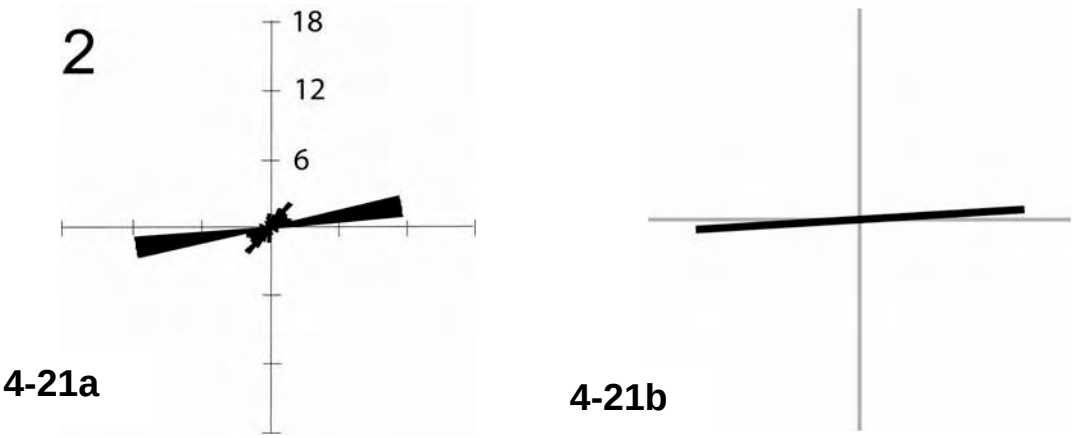

Figure 23. Grid cell 2 is an example of unimodal orientation. Figure 23a is the rose diagram for grid cell 2. After statistically analyzing grid cell 2, one orientation is preferred (Figure 23b). If fractures controlled flow in this portion of the aquifer, the result would be a preferred east-west flow direction.

4.2.3.2 Bimodal

Bimodal orientations indicate the presence of more than one orientation. Bimodality may have more than two preferred orientations, two weak orientations, or a preferred and a weak orientation (Figure 24).

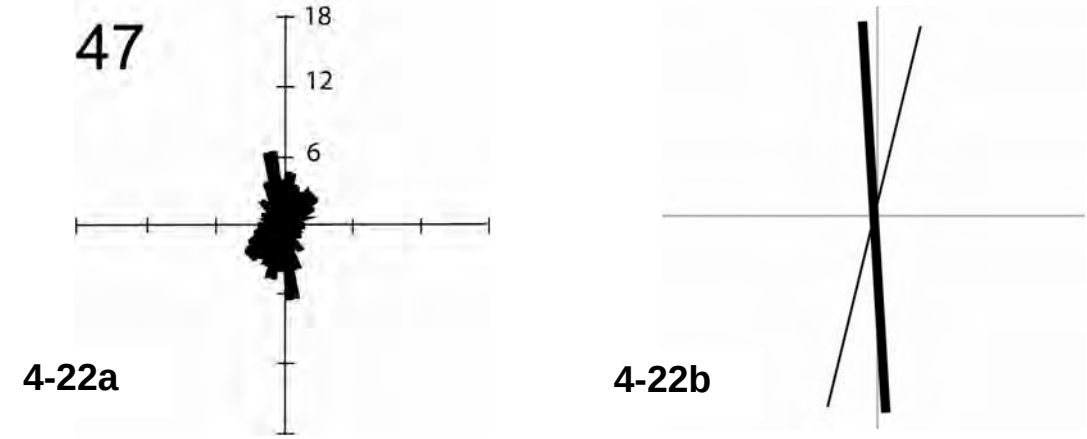

Figure 24. Grid Cell 47 is an example of bimodal stream orientations over the study area. Figure 24a is the rose diagram for grid cell 47. After statistical analysis one preferred orientations is found and one weak orientation (Figure 24b).

4.2.3.3 Polymodal

Polymodal behavior is a distinctive behavior in which many dominant orientations are distinguishable. After conducting the statistics on grid cell 62 we find that it is polymodal (Figure 25). One strong orientation is present and two weak orientations are orthogonal to the strong signal.

The areas that show polymodal orientations are dominantly in highly faulted areas. Faults and fractures are influencing the polymodal characteristics. Both open and closed faults and fractures are present and are creating conduits and barriers to flow. A more detailed analysis of each grid using water chemistry and electrical conductivity methods it will be help determine more detailed flow paths within a grid cell.

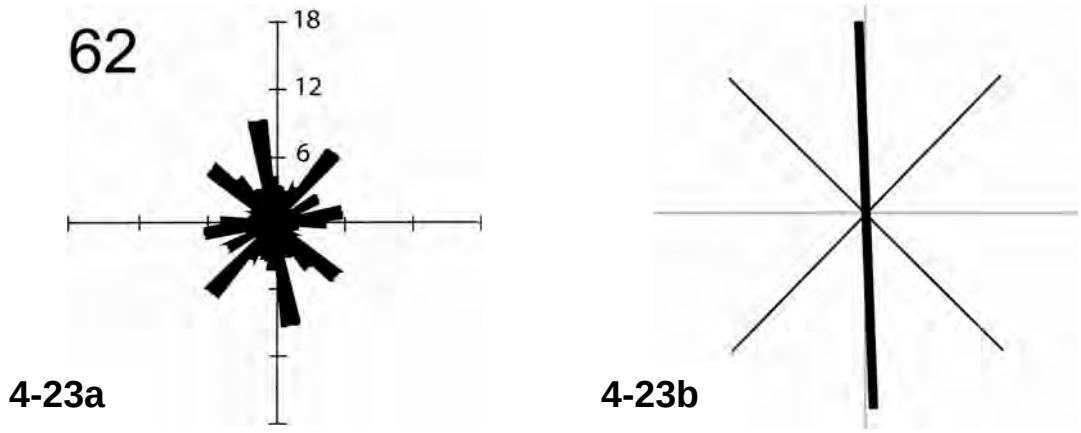

Figure 25. Grid Cell 62 is a good example of polymodal stream orientations. In Figure 25a it is difficult to determine if a preferred orientation exists. After calculating the statistics it is evident that it is polymodal (Figure 25b).

4.2.4 Statistics

All rose diagrams for streams were statistically analyzed for both the 10-km grid cells and the 2.5 km grid cells. The faults were analyzed only at the 10-km scale because at a higher resolution there would be a lack of sufficient data for analysis. After completing the statistics on each of the rose diagrams, the strong and weak orientations were plotted over the study area (Figure 26).

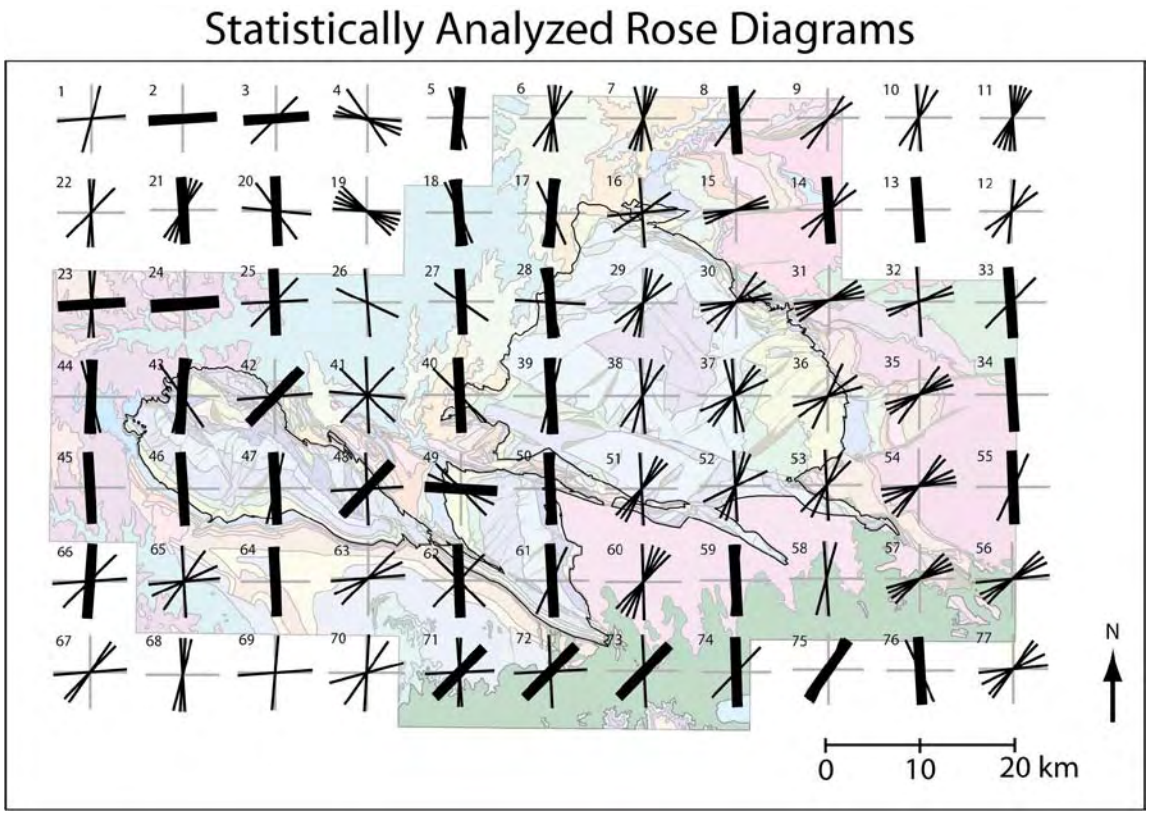

Figure 26. The 10x10 kilometer streams grid cells map for streams are statistically analyzed and plotted over the study area. Strong signals are indicated by the dark black line, and weaker signals are indicate by a thinner black line.

A more detailed statistical analysis over the Hunton Anticline using the 2.5-km grid cells shows some interesting features (Figure 27). The higher resolution grid cells support the north-south trends being seen in the streams and faults. In the Oil Creek formation (Ooj), streams are not present. The lithology of the Oil Creek formation is a sandstone, which is very friable, porous, and permeable. There may be fewer streams in this area due to these characteristics.

The GIS faults layer was studied to determine what preferred orientations can be seen (Figure 28). The data layer for the faults is much smaller than the streams due to the number of faults in the study area. This explains why some grid cells do not have any data.

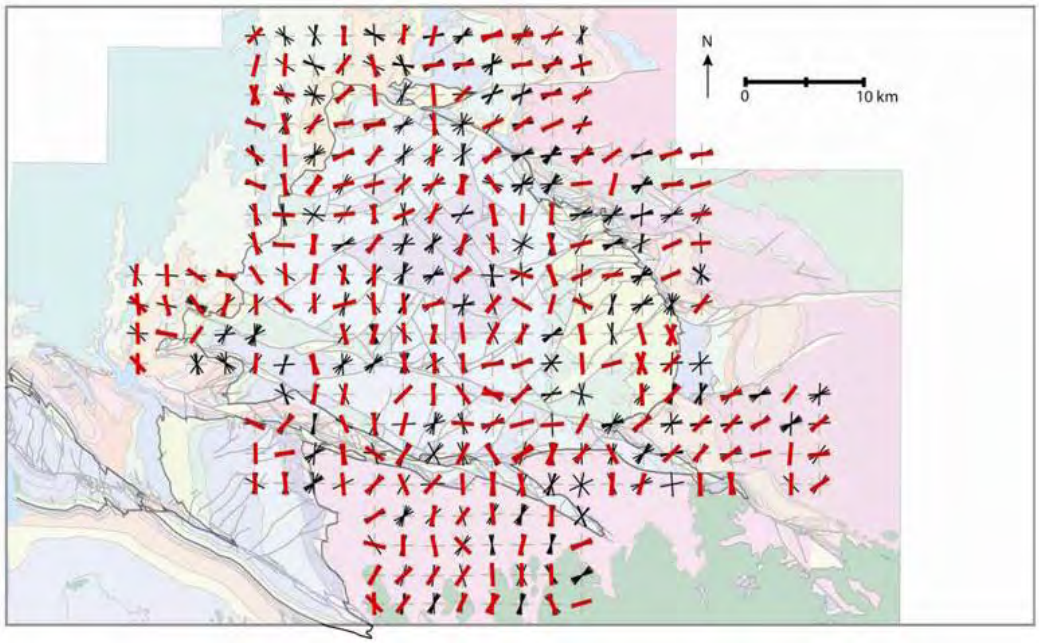

Figure 27. Statistically analyzed 2.5 x 2.5 grid cells over the Hunton Anticline. The thick red lines indicate strong signals; the black lines indicate weak signals.

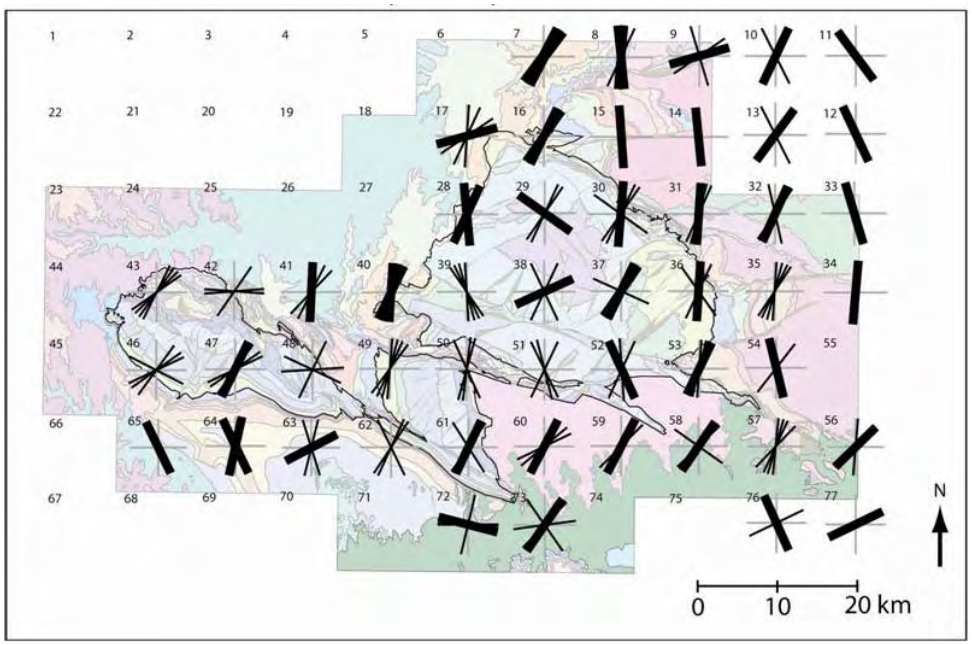

Figure 28. The preferred fault orientations of statistically analyzed faults. The overall preferred orientations are much more difficult to see using this map, however they do not follow the preferred west to northwest orientation found by Marshak (2003) evaluating regional-scale tectonics.

4.2.5 Field Work and Stream Data Correlation

The field work conducted over the study area was compared to stream and fault data in that grid cell. The grid cells field work was conducted in was 37, 59, and 47. There is a correlation between field work and stream data for grid cells 37 and 47. Though a direct correlation cannot be made between stream and faults using figure 29, a histogram of orientations for streams and faults indicates a correlation between the two using figure 30.

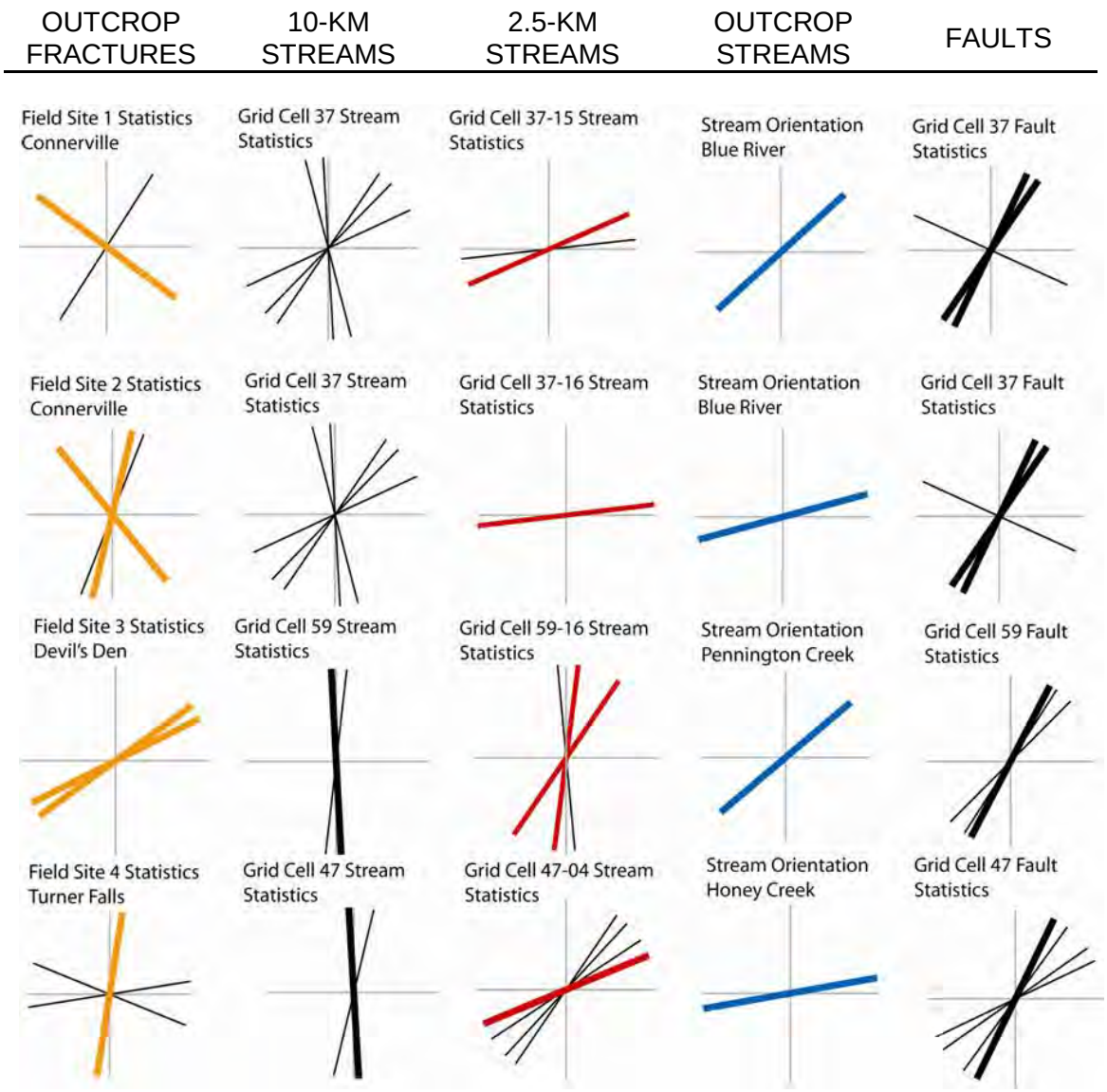

Figure 29. A comparison of orientations using outcrop, stream, and fault data.

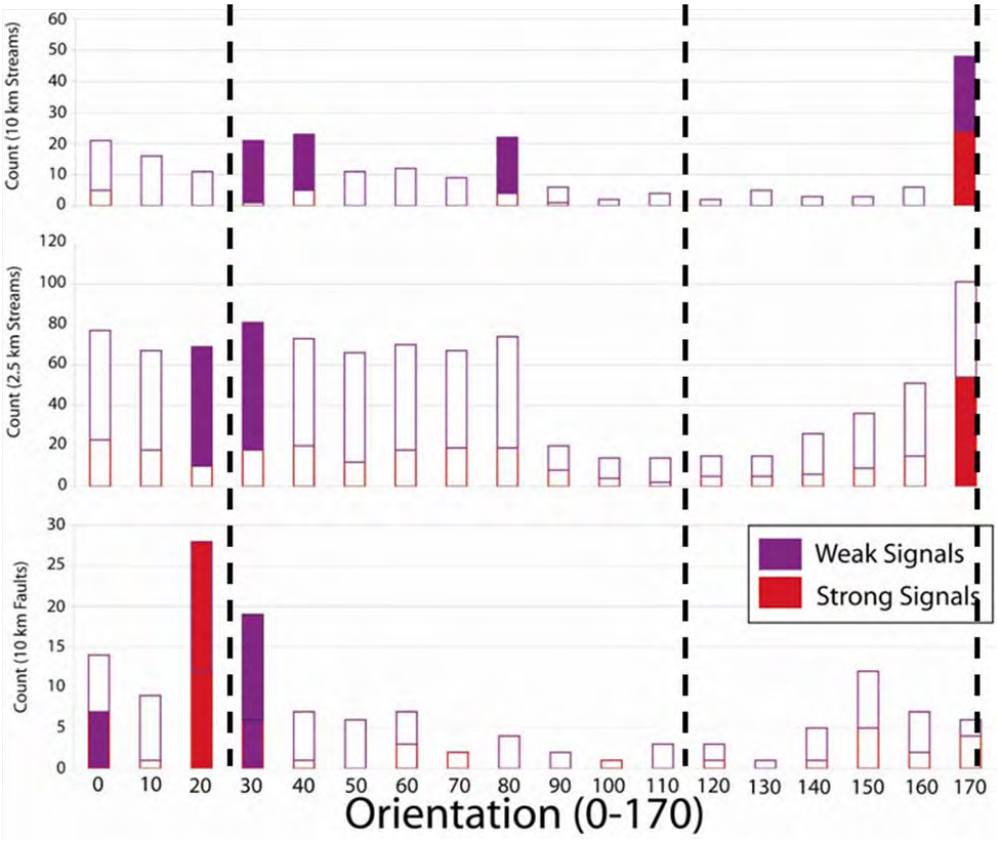

Figure 30. A histogram of the 10 stream orientations shows preferred orientations of 0° and 170° and a 20° and 30° trend. Other orientations are present, such as the primary fault trend of 115°, but are not as dominant this would be expected in an area with a complicated structural history such as the Arbuckle-Simpson Mountains. The orientations of the 2.5-km streams and faults also indicate a preferred orientation similar to the 10-km stream layer.

By creating a histogram of the streams and faults it is evident that the streams and fault have similar trends. Figures 31 and 32 are used to better visualize the extent the preferred orientations over the aquifer. The grid cells are colored for strong and weak orientations of 0° and 170°. Figure 26 grid cells are colored for 20° and 30° orientations. Potential flow lines for the aquifer can be determined by observing these trends and using the potentiometric map of the area to aid in the analysis. The GIS streams layer also shows a preferred orientation of 0° and 170° degrees (Figure 33). Another map for the preferred orientations of 20° and 30° is provided as well (Figure 34).

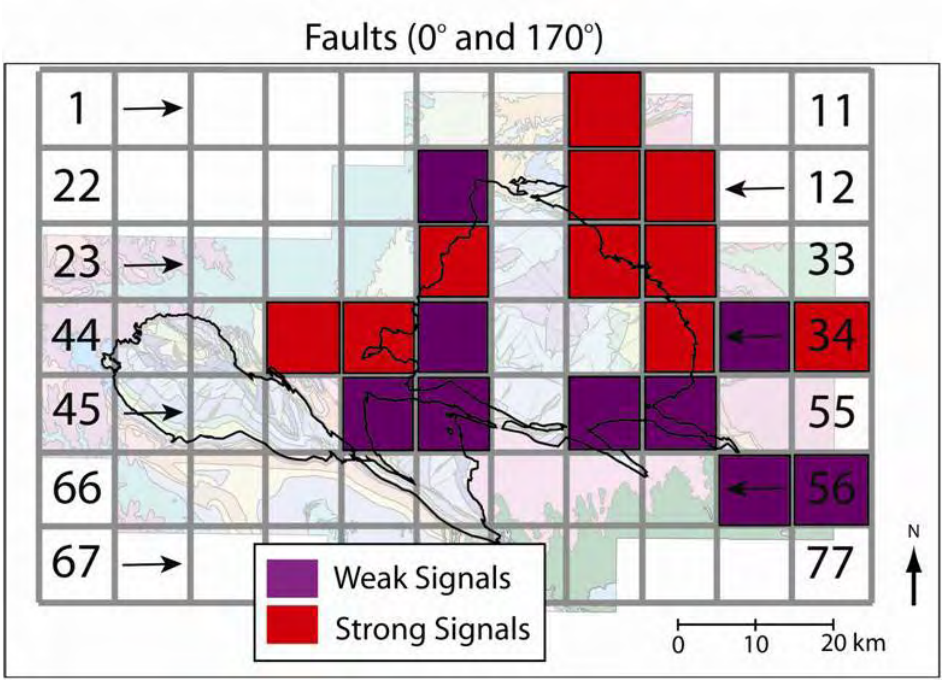

Figure 31. The GIS fault layer is used to determine if a correlation exists between streams and faults. The GIS fault layer has less bias than the streams layer due to digitizing techniques.

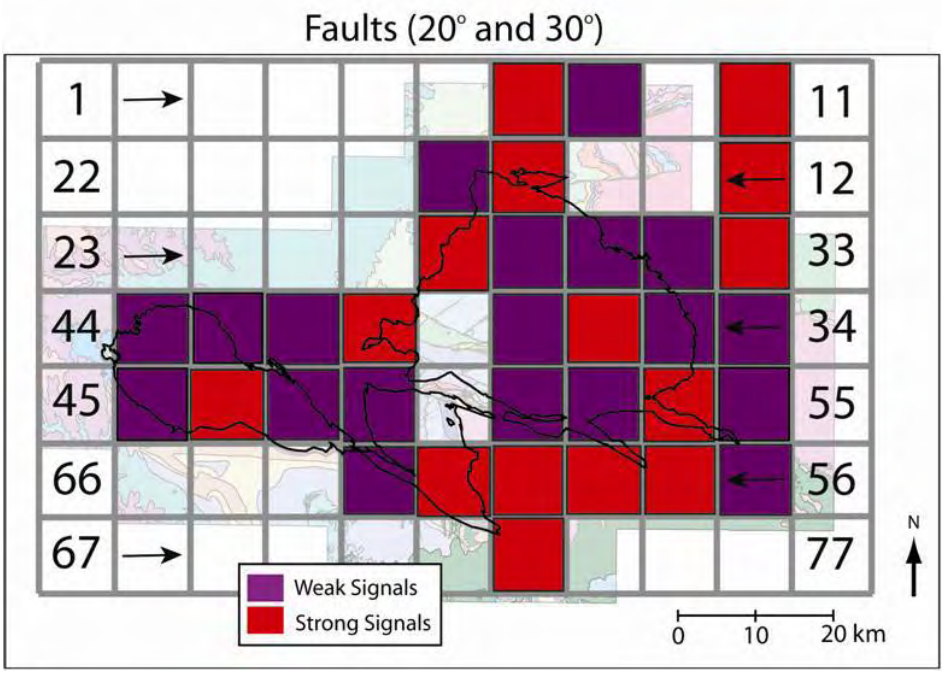

Figure 32. The GIS fault layer is used to determine if a correlation exists between streams and faults. This map is for strong and weak signals at 20 and 30 degrees.

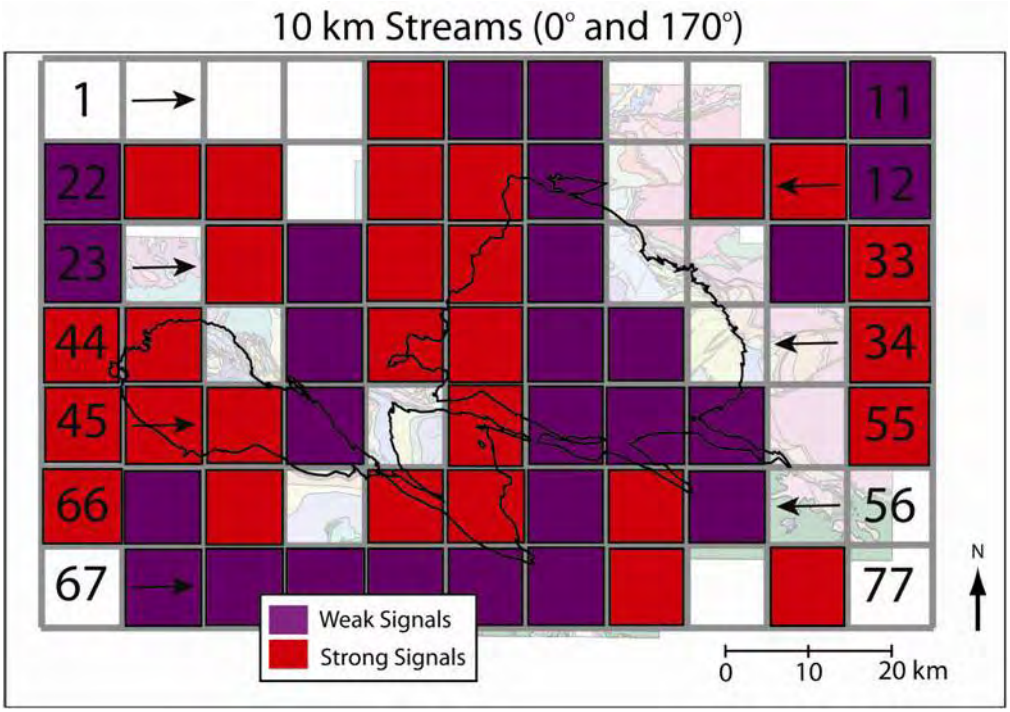

Figure 33. The GIS stream layer is used to determine if a correlation exists between streams and faults. This map is for strong and weak signals at 0 and 170 degrees.

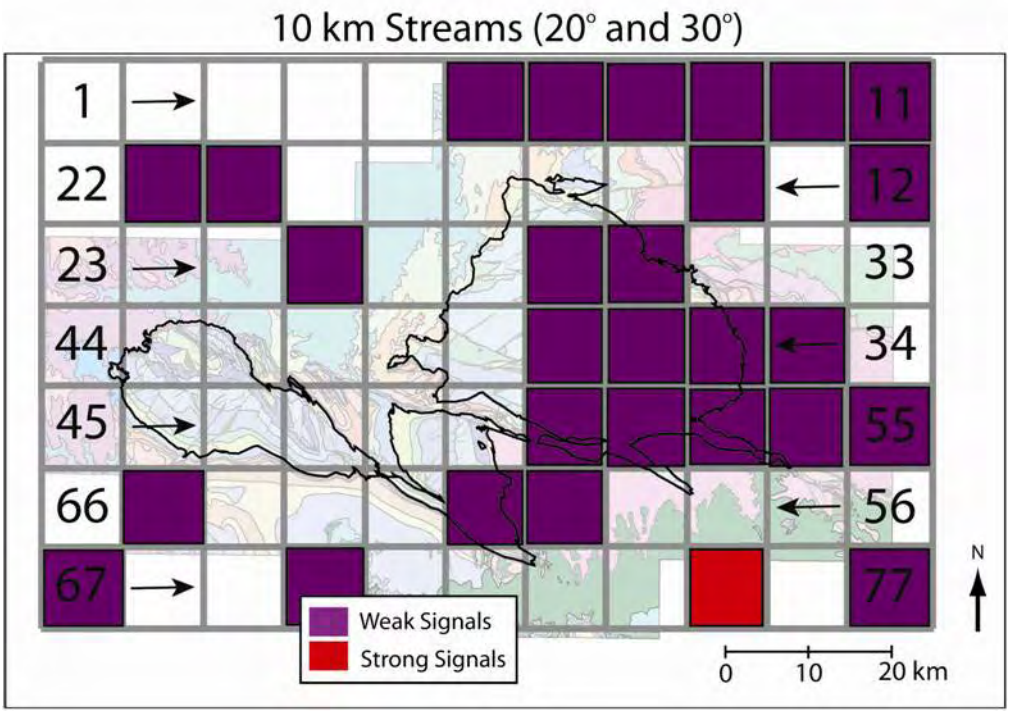

Figure 34. The GIS stream layer is used to determine if a correlation exists between streams and faults. This map is for strong and weak signals at 20 and 30 degrees.

4.2.6 Anisotropic Flow Net Analysis

Hypothetical anisotropic flownets were created for the 0 degree and 25 degree preferred orientations observed in the stream and fault data. These allow a regional understanding of flow direction under a range of possible fracture controls on the system. The flownets were also modeled for isotropic conditions and anisotropy parallel to the major faults at 115 degrees. These demonstrate similar characteristics for the aquifer. The model boundaries are not well constrained, so the steep gradients near the boundaries can be discounted.

The isotropic flownet for the aquifer shows convergent flow for many of the creeks in the aquifer and for Byrds Mill Spring (Figure 35). This would be expected for a dolomitic karst aquifer, and would be indicative of fracture or conduit control over the lower reaches of the streams or the flowpath leading to Byrds Mill Spring. The notable exception is the Blue River, which does not even appear to influence the water table in the area. The major faults in the aquifer do not appear to be major barriers to flow, although the magnitude of the gradient does vary near some faults, with the magnitude increasing the most near the boundaries of the aquifer where the Simpson overlies the Arbuckle.

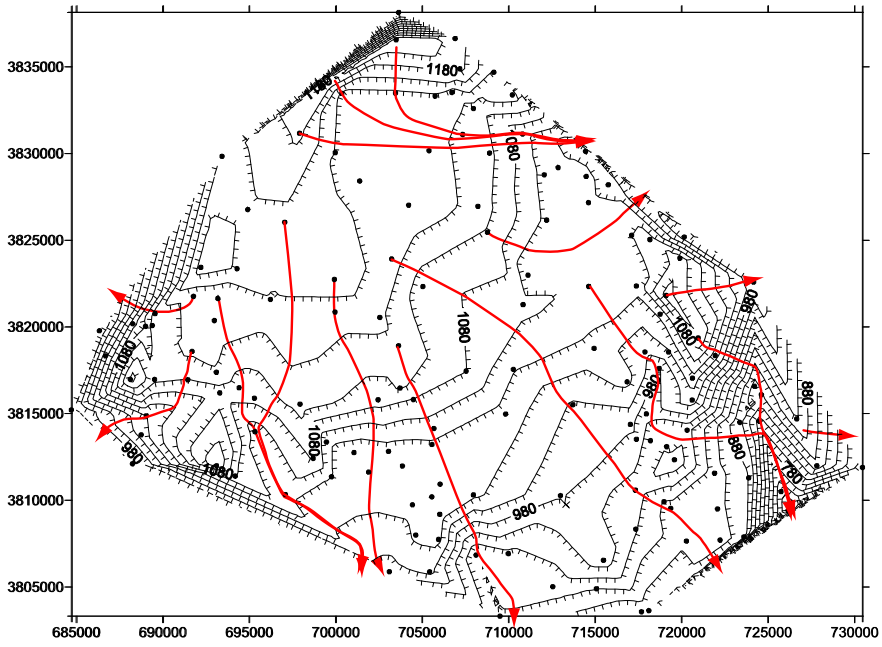

Figure 35. Isotropic flow net for 1995 USGS synoptic data in UTM coordinates. Black hashed lines represent modeled groundwater equipotentials in feet amsl. Red lines indicate the direction of flow assuming isotropic conditions. Steep gradients at boundaries are associated with a lack of data control, not with geologic conditions.

A strong north south anisotropy induced by fractures which appear to control the surface water orientation leads to a similar result as the isotropic system (Figure 36). The primary difference from isotropic conditions is the larger capture zone for Byrds Mill Spring. The influence of north-south anisotropy would also cause some northward flow towards the spring from the eastern margin of the aquifer.

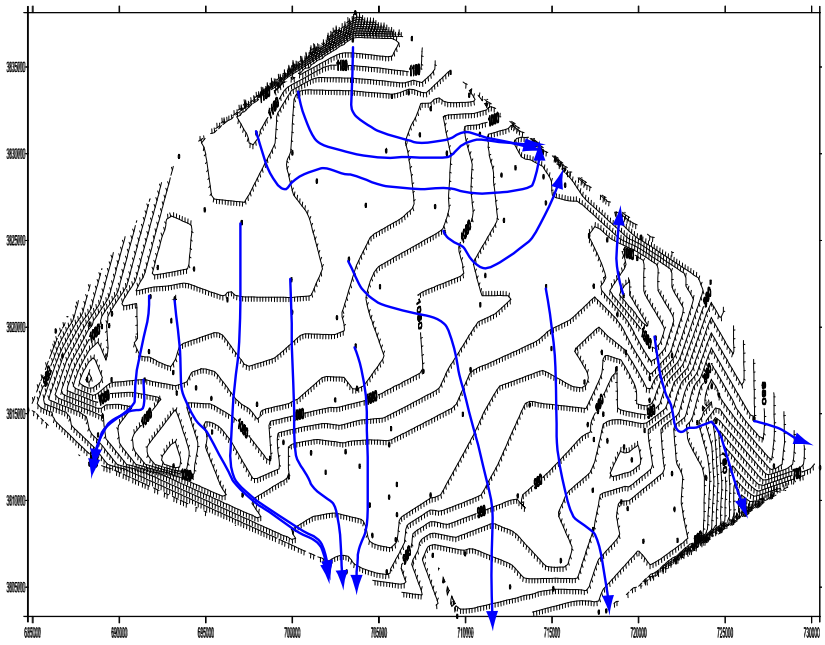

Figure 36. Anisotropic flow net for 1995 USGS synoptic data assuming an anisotropy ratio of 3 (K_H/K_L=9) and a preferred orientation of 0° (north-south stream and fault orientation). Black hashed lines represent modeled groundwater equipotentials in feet amsl. Blue lines indicate the direction of flow assuming anisotropic conditions. Steep gradients at boundaries are associated with a lack of data control, not with geologic conditions.

A preferred orientation of 25 degrees causes significant changes in the flow pattern for the aquifer (Figure 37). The flow lines largely head towards the southeast with little convergence in the flowlines. The orientation largely eliminates Byrd Mill Springs as a discharge feature, with a flow path only coming from the south along the eastern margin of the aquifer.

If the preferred orientation of the major faults (115°) dominated the flow system, significant differences would exist in the groundwater flowfield (Figure 38). Discharge would largely be to the east and west with few flowlines heading towards the southern discharge areas. The flownet appears to give a result that largely avoids the Blue River.

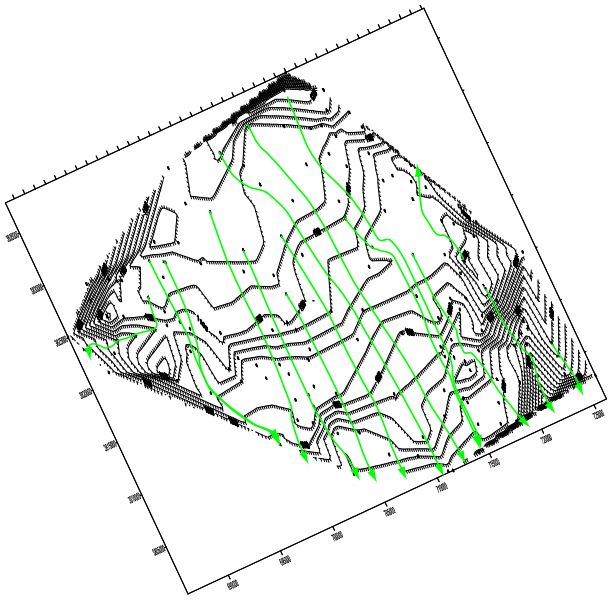

Figure 37. Anisotropic flow net for 1995 USGS synoptic data assuming an anisotropy ratio of 3 (K_H/K_L=9) and a preferred orientation of 25° (stream and fault orientation). Black hashed lines represent modeled groundwater equipotentials in feet amsl. Green lines indicate the direction of flow assuming anisotropic conditions. Steep gradients at boundaries are associated with a lack of data control, not with geologic conditions.

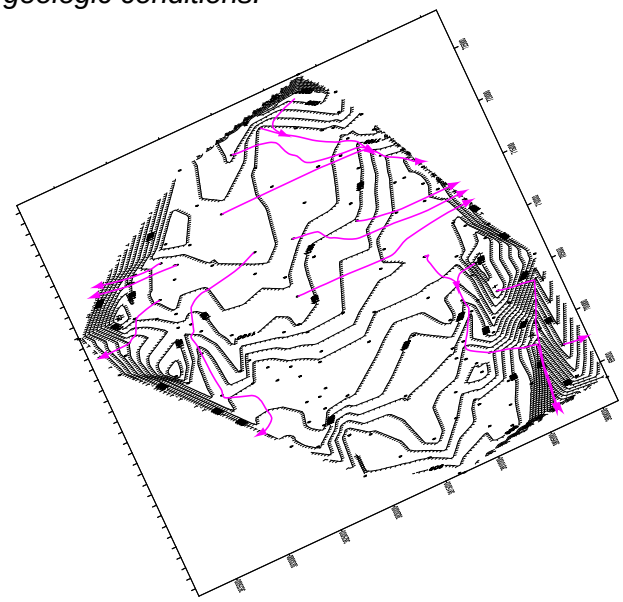

Figure 38. Anisotropic flow net for 1995 USGS synoptic data assuming an anisotropy ratio of 3 (K_H/K_L=9) and a preferred orientation of 115° (aligned with major faults). Black hashed lines represent modeled groundwater equipotentials in feet amsl. Pink lines indicate the direction of flow assuming anisotropic conditions. Steep gradients at boundaries are associated with a lack of data control, not with geologic conditions.

When comparing the range of possible dominant fracture directions, some generalities are noted. Convergent flow is observed for most of the orientation in the streams and at Byrds Mill Spring except for the Blue River (Figure 39). The southern portion of the aquifer does not appear to be strongly affected by anisotropy since the orientations of the flowlines have little change under the different scenarios, so anisotropy is unlikely to affect groundwater models of the aquifer in the southern areas. The northern portion of the aquifer is strongly influenced by anisotropy causing significant changes in direction depending on which fracture orientation is dominant for the region. An groundwater models will need to evaluate anisotropic effects in these areas if calibration is difficult. Additionally, for understanding well capture zones, or contaminant flowpaths, the northern area will need further study.

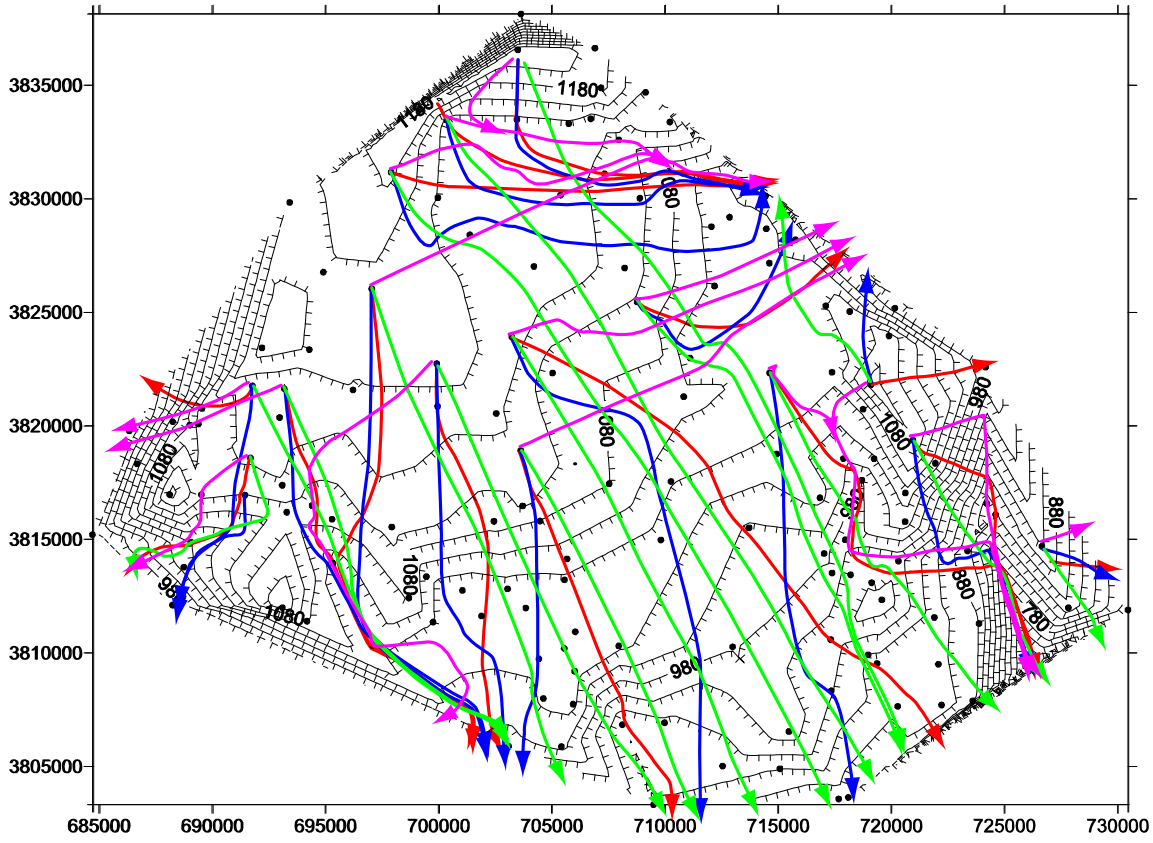

Figure 39. Model flow net for 1995 USGS synoptic data comparing hypothetical isotropic and anisotropy ratios of 3 (K_H/K_L=9) with preferred orientations of 0°, 25°, and 115° in UTM coordinates. Black hashed lines represent modeled groundwater equipotentials in feet amsl. Colored lines indicate the direction of flow assuming a preferred orientation. Steep gradients at boundaries are associated with a lack of data control, not with geologic conditions.

4.2.7 Hydraulic Data

On the regional scale, fracture and hydraulic data provide insight into the hydraulics of the surface and groundwater of the Arbuckle Simpson aquifer. On the regional scale, the streams over the Hunton anticline are dominated by the strong north-south orientation seen in the data. Many of the streams trend roughly 170 degrees from north (Figure 40). While the major fault orientation of 115 degrees from north is not strongly evident in the fracture and faulting dataset, it is apparent in the surface streams and appears to control the location of a portion of the northern Blue River, and the location of Byrds Mill Spring (Figure 40).

In evaluating any potential hydraulic connections between Byrds Mill Spring and Blue River, hydraulic data collected as part of the Arbuckle Simpson Hydrology Study provides insight. While the USGS record for Blue River discharge at Connerville varies by a factor of 300 over the period of record (21 – 6330 cfs; 0.59 – 179 cms), the discharge of Byrds Mill Spring varies only by less than a factor of 10 (4.6 – 43 cfs; 0.13 – 1.2 cms) (Figure 41). If the data from the Blue River are limited to data with a specific conductivity greater than 530 mS/cm to remove storm pulses, a significant correlation exists between the two datasets (R^2=0.59) (Figure 42). The data for the Blue River occasionally go well above the values the relationship would predict, but the values for Byrds Mill Spring appear strongly governed by the relationship. This is what would be expected for Byrds Mill Spring acting as an underflow spring for the Blue River. The connection between the two systems would likely occur along the 115 degree trend observed at the surface (Figure 40), but can only be confirmed through groundwater tracing.

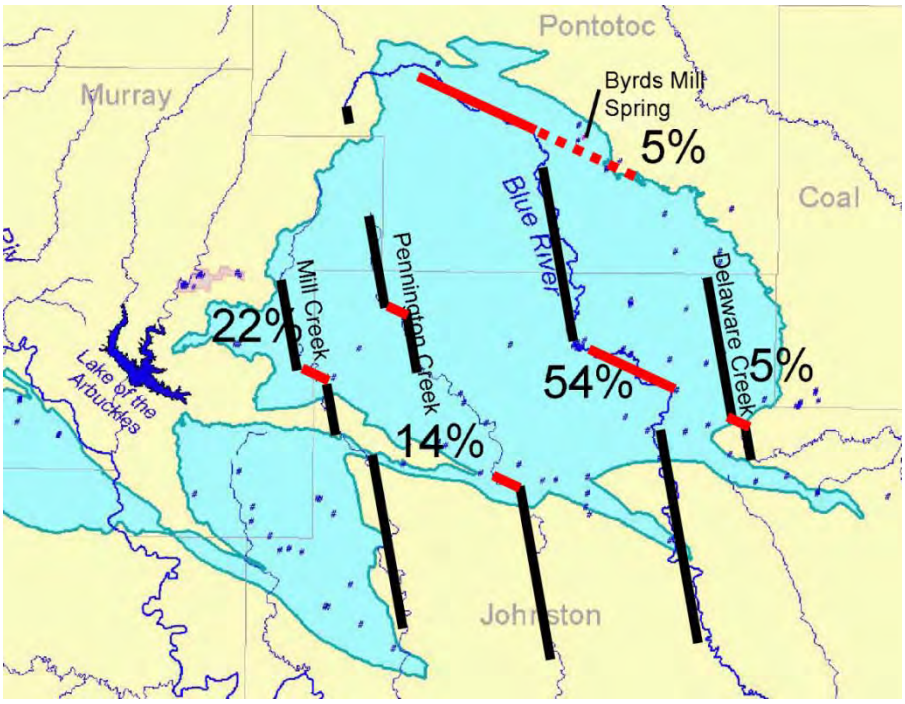

Figure 40. Map of the Hunton anticline demonstrating strong trends in creek orientations at 170 degrees from north (in black) and 115 degrees from north (in red).

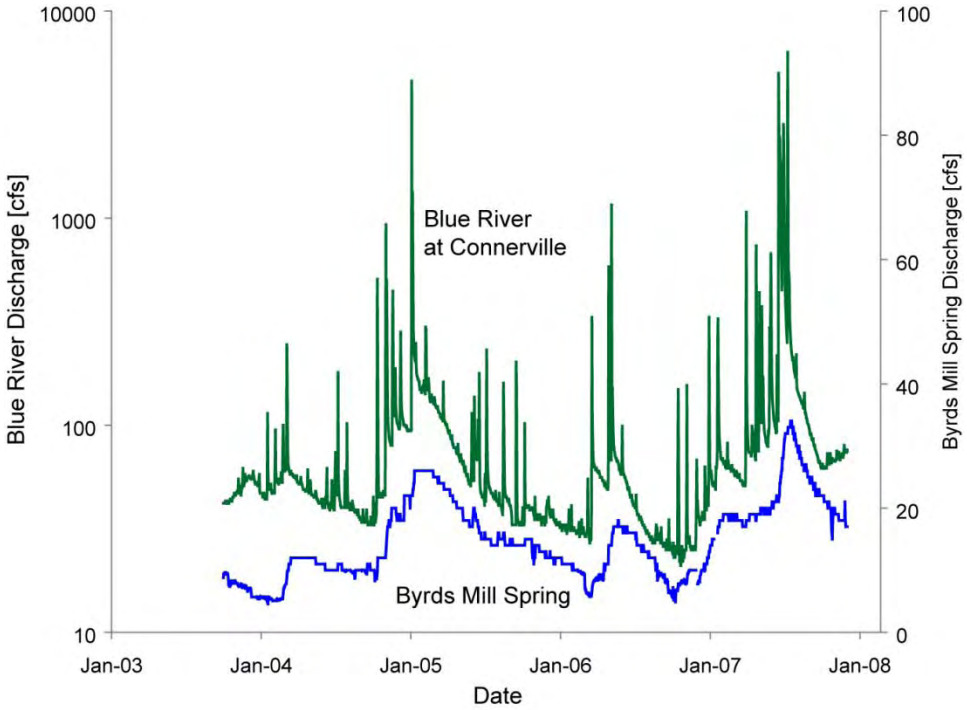

Figure 41. Discharge records for Blue River at Connerville and Byrds Mill Spring. Note that the axis for the Blue River is logarithmic while the axis for Byrds Mill Spring data is linear.

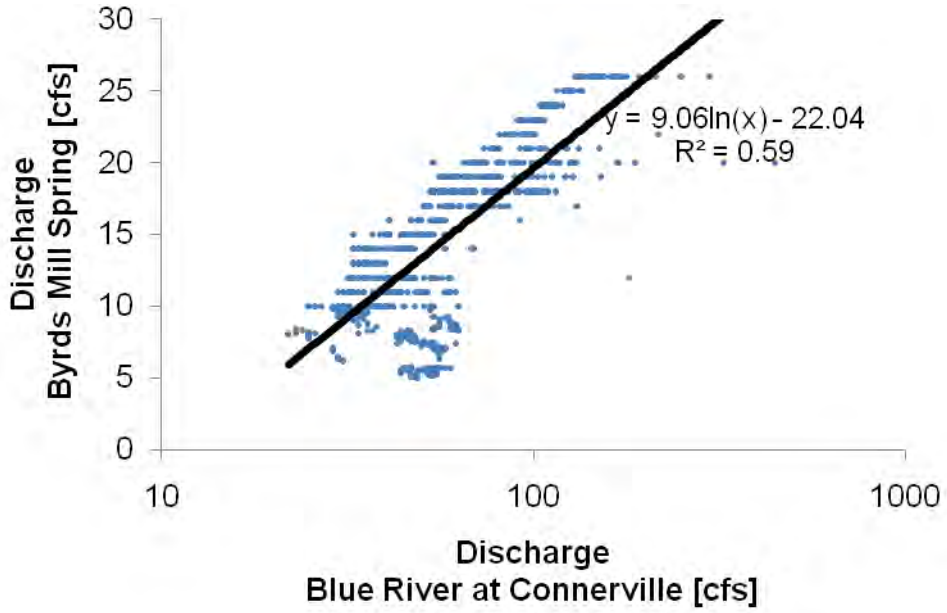

Figure 42. Correlation between Blue River at Connerville discharge data and Byrds Mill Spring data for EC at Blue River greater than 530 mS/cm. This relationship demonstrates that Byrds Mill Spring is likely an underflow spring for the Blue River.

Local groundwater gradients are similar to the regional groundwater gradients, but connections between groundwater and surface water may be limited at particular locations. The well and stream elevation data at the Spears Ranch indicate that the aquifer is discharging to surface water at this location, but the relationship between groundwater elevations and surface water elevations is not extremely strong, especially during storm events (Figures 43 and 44). The initial data suggested that the relationship between the groundwater elevation at the well and the stream elevation was stronger, but once storm data were included, the relationship was shown to be weaker during storm events (Figure 44). Even under baseflow conditions, the relationship in not always consistently strong. This poor correlation between the Blue River and the nearby wells on the Spears Ranch indicates that the fracture network in the aquifer is not well connected in all locations. The gradients are approximately 0.02 m/m in the area, but will vary from 0.011-0.034 (Figure 45). This is a relatively high horizontal groundwater gradient for a fractured aquifer, indicating that horizontal connectivity is not strong.

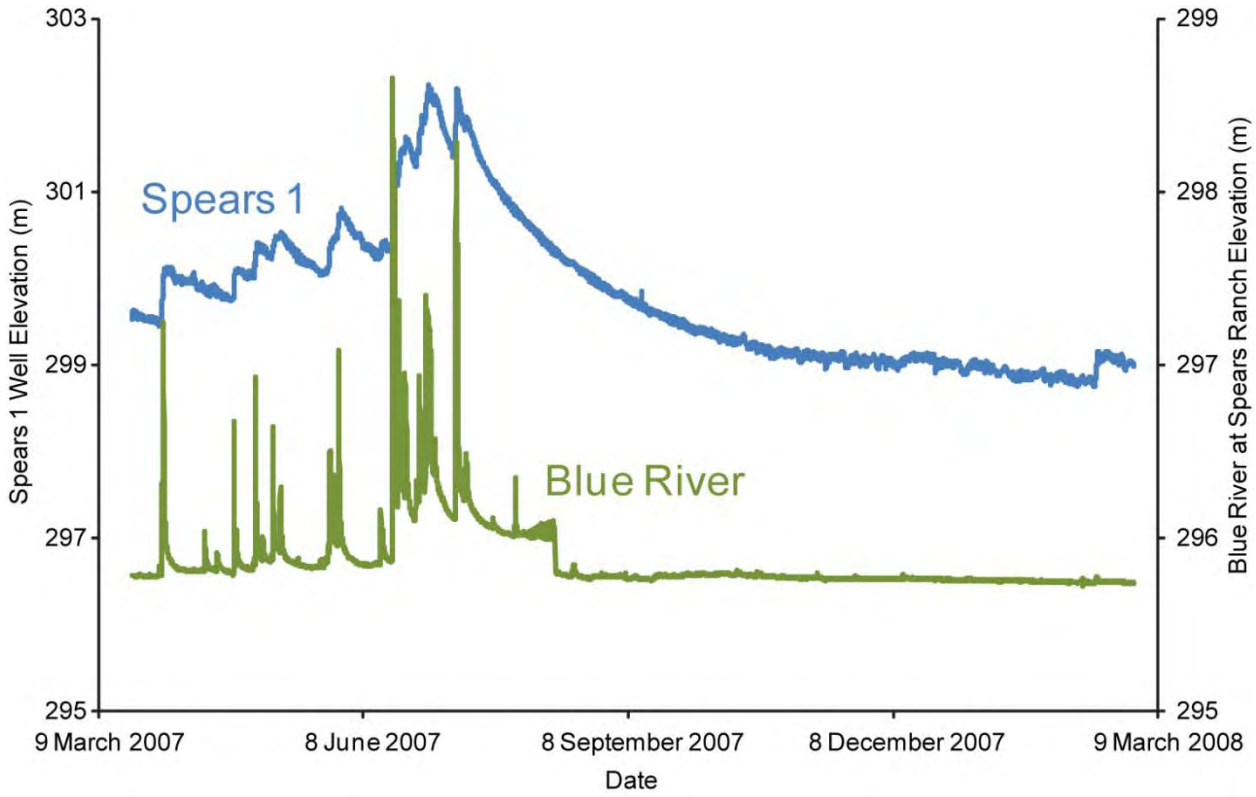

Figure 43. Water elevations in the Spears 1 well and the Blue River below the Spears Ranch dam.

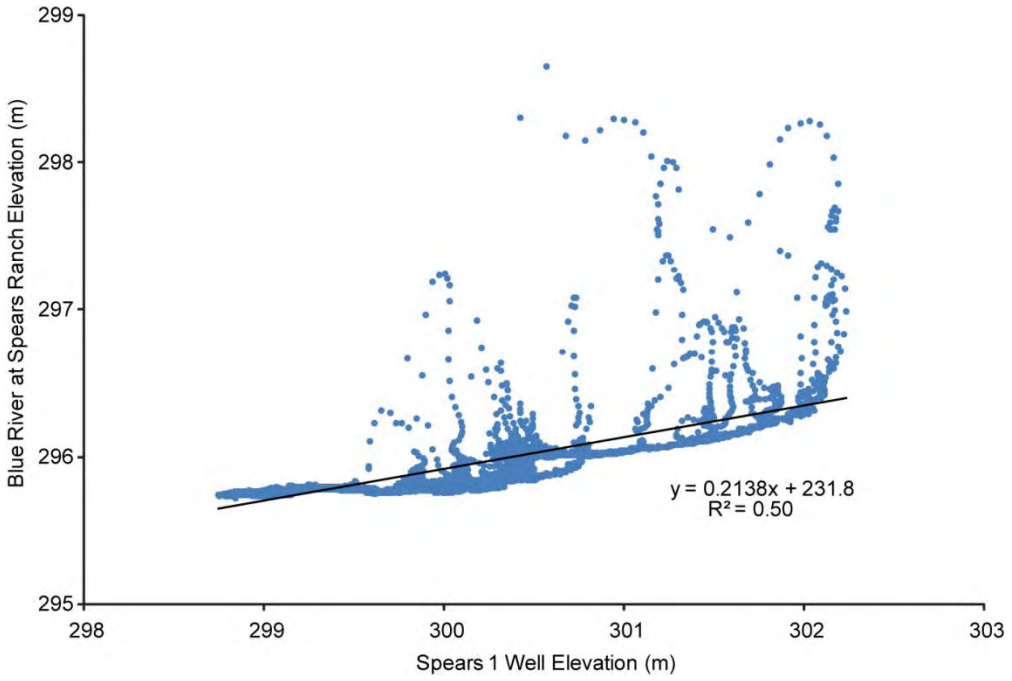

Figure 44. Relationship between the water elevation in the Spears 1 well and the Blue River water elevation.

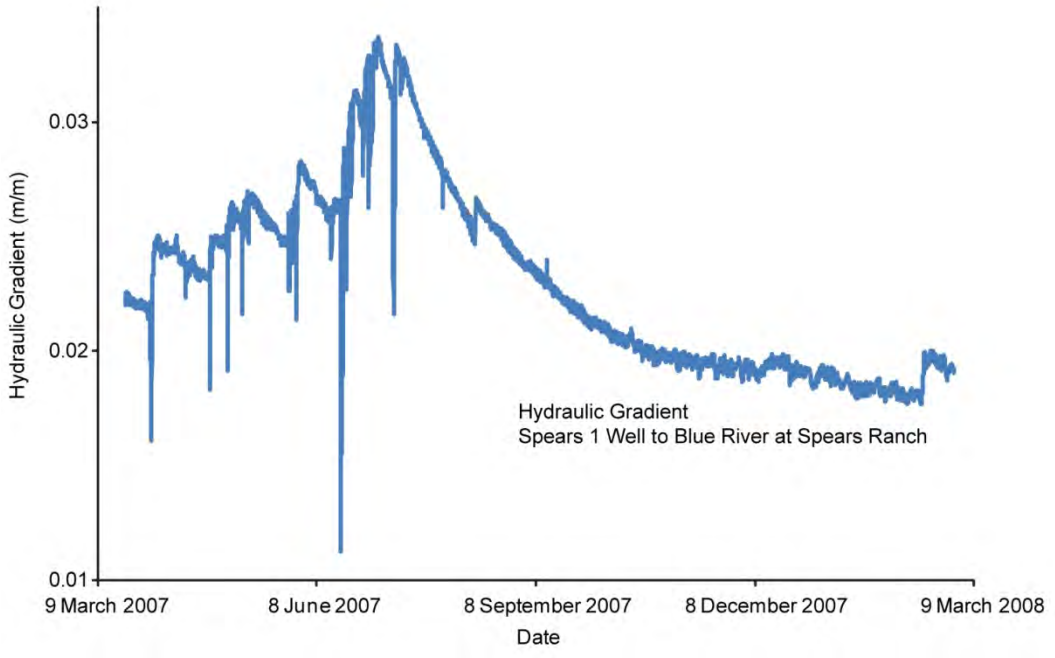

Figure 45. Hydraulic gradient between Spears 1 well and the Blue River at Spears Ranch (just downstream from the dam). Gradient is calculated with a distance of 170 meters between the locations.

4.3 Discussion

The primary issues that can be resolved with an analysis with horizontal fracture data are the primary orientations that may control flow in the aquifer, the possible presence of conduits in the aquifer, and controls on aquifer connectivity. Three orientations appear to be present in the fault and stream data analyzed. The strong fault orientation at 115° from north is not present as a significant signal in the stream and fault data (Figure 30), but it obviously influences a portion of the surface water network (Figure 40). This trend appears to provide a connection between the orientation of the Blue River and Byrds Mill Spring. While this orientation predict strong east and west flow directions for the aquifer, which contradicts the primary discharge to the south (Figure 38), it still may exert some control on flow directions. The overlying Simpson formation in the east may cause discharge to occur at the Blue River due to a permeability boundary, not through horizontal fracture control. This makes it possible that the Blue River is strongly fed from the west through this fracture network, but this would only be proven through additional evidence.

The fault and stream orientation at 25 degrees from north (orthogonal to the major faults) provides the strongest orientation signal in the fault data and a strong signal in the stream data (Figure 30). The surface streams do not appear to be strongly controlled on a regional scale by this orientation (Figure 40). This orientation would generate a much different flow interpretation in the northern area of the aquifer (Figure 39), suggesting much of Byrds Mill Spring flow comes from the eastern edge of the aquifer from northern and southern flowpaths. As all other orientations tested indicate a convergent flow path along the 115° orientation for Byrds Mill Spring, and the relationship that exists between the spring and Blue River, it is not expected that this is a controlling fracture orientation on a regional basis. However, on a local scale, it may provide controls over flow directions.

The final strong orientation present dominantly in stream orientation data is a roughly north-south orientation that exerts significant control over surface water direction over the aquifer (Figures 30 and 40). This orientation provides a groundwater flow net interpretation that is consistent with most of the discharge features for the aquifer (Figure 36). As the surface

water also is dominated on the regional and local scale by this orientation, it may provide the direction for regional anisotropy in the aquifer.

All stream and fault orientations that were evaluated, except for the 25 degree orientation, provide an indication of convergent flow for the surface water features and Byrds Mill Spring. The convergent flow interpretation is consistent across a range of possible anisotropy orientation and exists largely near the endpoints of the streams and Byrds Mill Spring (Figure 39). This may require high permeability flow areas to be added to any continuum models to reproduce this effect in the model. The obvious exception to this result is the lack of convergent flow for the Blue River. The location of the river may be controlled by the orientation and location of fractures, but the amount of discharge is likely controlled by permeability limitation imposed by the Simpson overlying the Arbuckle in the eastern portion of the Hunton anticline.

The relatively strong horizontal hydraulic gradient across the aquifer does not appear to indicate significant fracture barriers to flow. The Simpson in the eastern portion of the Hunton anticline appears to alter the gradient, but the remaining fault system does not show significant evidence that the faults are barriers to flow. The strong gradient combined with the lack of strong changes in the gradient may be an indication that the flow is dominated by vertical flow vectors instead of the commonly assumed horizontal flow vectors.

5.0 Vertical Flow Evaluation

In the vertical orientation, geophysical methods are compared against each other to determine if a consistent pattern is present among the various techniques. The results of the geophysical methods are compared against temperature data with depth to evaluate correlations.

5.1 Methods

The methods used for this analysis is largely compiling the data from a number of projects that were ongoing as part of the Arbuckle Simpson Hydrology Project. The data are analyzed for evidence of vertical fracturing.

5.1.1 Geophysical Data

A number of different geophysical methods have been used to evaluate the Arbuckle Simpson aquifer. Gravity, electrical resistivity (ERI), seismic, and helicopter electromagnetic (HEM) have been applied. These vary in the range of depth that the methods can observe with the seismic approach allowing the deepest evaluation of the aquifer. The gravity and seismic methods are the only ones that are evaluated that can get some information down to the basement rocks (~1000 meters deep). All of the methods have been applied over faulted areas allowing an evaluation of the vertical distribution of faulting and fracturing in the aquifer. The data evaluated for this report include gravity data collected over faults in the area (Scheirer and Scheirer, 2006), electrical resistivity data of faults (Riley, 2007), seismic data analyzed for vertical fracturing (Kennedy, 2008), and helicopter electromagnetic data (Smith et al, 2008).

This report relies on the interpretation of the individual authors to determine if they thought their data showed vertical fracturing of the aquifer. As geophysical datasets are nonunique in most cases, correlation among the datasets and interpretations are used instead of relying on a single technique.

5.1.2 Borehole Logs

Borehole data were available as a temperature log collected by U.S. EPA at the Spears 2 well site. As this data were from a newly drill open hole well, the aquifer has not fully equilibrated due to vertical flow. As these data were unexpected for the aquifer, the log was recollected, and packer tests were performed at fracture locations to test the temperature of the well in discrete constrained intervals. These data were collected over the 1800-foot range of the well. Additionally, bottom hole temperature data were available for a set of wells in the aquifer (Puckette et al., 2009). These temperature data were compared with common geothermal gradients to observe any significant anomalies in the trends.

5.1.3 Well and Spring Temperatures

Well and spring temperature data are available for the aquifer to compare to the borehole temperature data collected from logging or drilling. The temperature data from wells and springs have been compiled by Cole (2006). The dataset is limited. Data are also available from well chemistry sampling detailed by the USGS (Fairchild et al, 1990; Christensen et al, 2008). The temperature data were evaluated for trends that may indicate vertical flow processes. The relationship between the temperature data and an expected normal geothermal gradient of 15 – 25 degrees per kilometer was evaluated.

5.2 Results

The results indicate a consistent pattern of strong vertical fracturing in the aquifer. The results indicate that little to no positive geothermal gradient exists in the aquifer. The geophysical results are presented followed by the results from the temperature data.

5.2.1 Geophysical Data

Geophysical data collected over the Arbuckle-Simpson aquifer included gravity, electrical resistivity, seismic, and helicopter electromagnetic methods. The geophysical data indicate some consistent results when evaluating the vertical fracturing of the aquifer. The major faults appear to be steeply dipping in all methods applied. Fault orientation was quantified using electrical methods (Riley, 2007). The features also appear consistent between methods (Smith, 2008) (Figure 46). The electrical evidence exists to a depth of 200 meters as a maximum, even though the aquifer may extend deeper than one kilometer. The gravity data (Scheirer and Scheirer, 2006) and seismic evidence (Kennedy, 2008) provide the only evidence that extends to basement depths at this time. The seismic data are in agreement with the other geophysical methods that the majority of fractures or contacts observed in the data are strongly dipping.

Conductive features in electrical resistivity imaging datasets also demonstrate shallow dipping features. These generally coincide with vertical faults and surface water features (Cemen et al, 2008). These ERI datasets indicate that the connections from the surface to vertical flow features at depth are limited in the extent and locations (Figure 47). For the image presented, the Blue River appears to simply be flowing over the top of the formation with the nearby springs acting as the regional discharge location which then feeds into the Blue River.

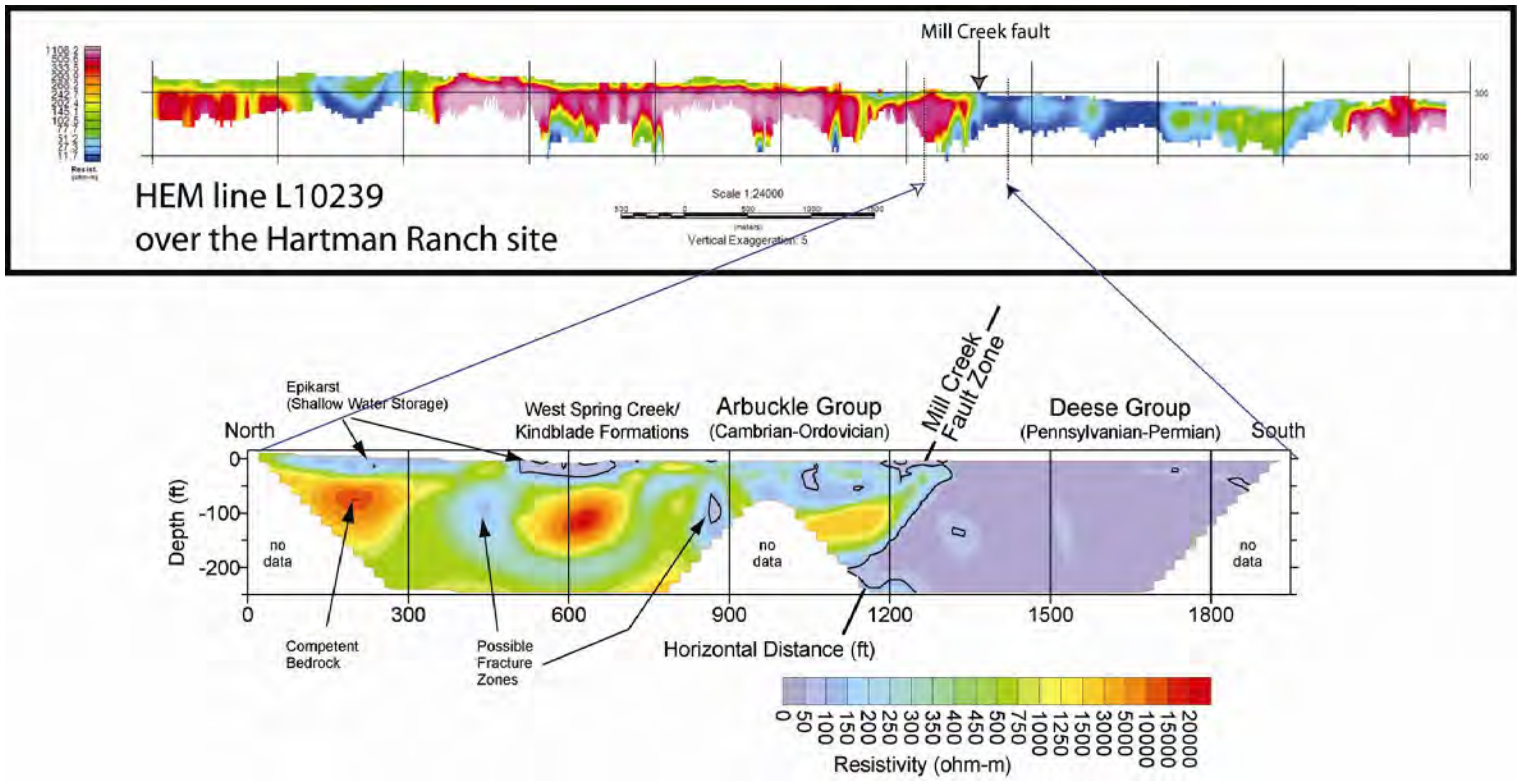

Figure 46. Comparison of HEM data and surface ERI data for Mill Creek Fault Zone (modified from Smith et al, 2008).

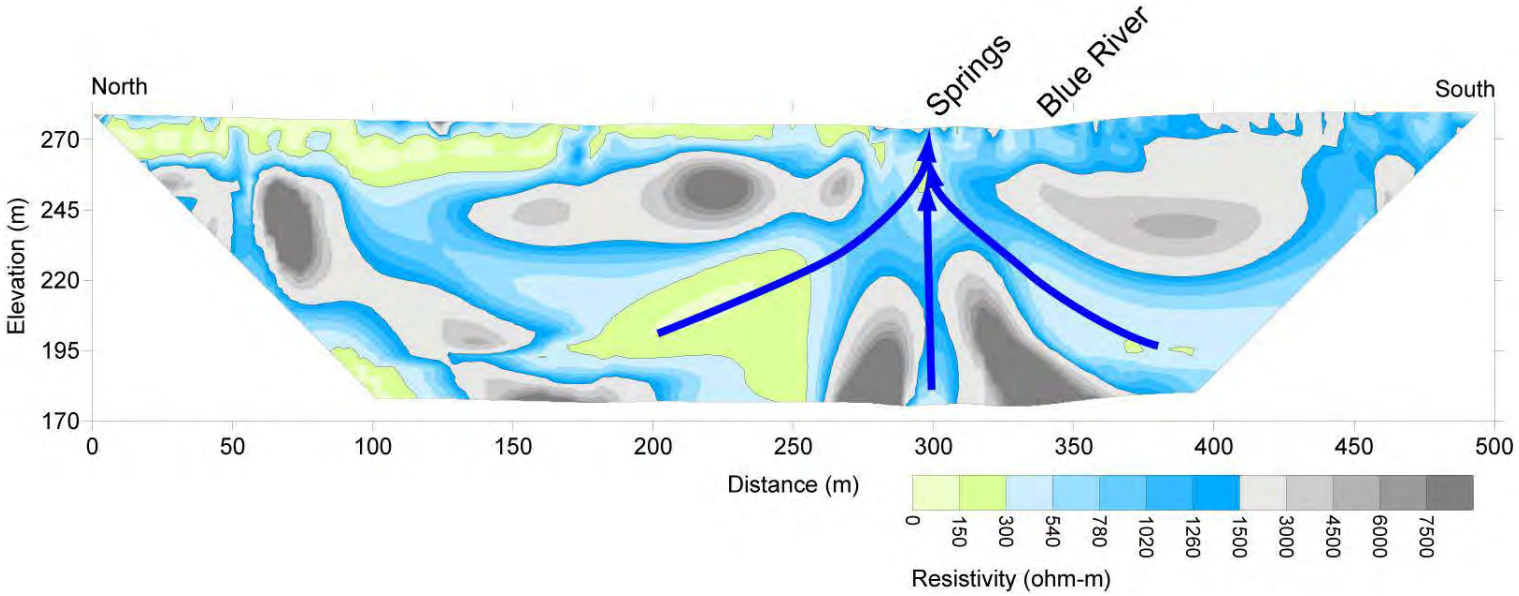

Figure 47. Electrical Resistivity data perpendicular to the discharge zone of Washington Springs (at Arbuckle-Simpson Ranch) crossing the Blue River (modified from Cemen et al, 2008). The conductive features in the dolomite align with surface water discharge at Washington Springs.

5.2.2 Temperature Data

Temperature data in the Arbuckle Simpson aquifer show two distinct trends. Data from petroleum wells in the area show a consistent geothermal gradient of 15.2 degrees Celsius per kilometer (Table 1; Figures 48 and 49). The data extend over a depth range from 187 – 2736 meters (613 – 8978 feet) and a temperature range from 26.7 – 55 C (80 – 131°F). This trend is fit with a linear trend line with a goodness of fit of 0.84 (Figure 48) If extrapolated to the surface, they would predict a surface discharge temperature of 24 C (75°F), however it must correspond to approximately the average annual temperature, so a concave fit is more physically realizable (Figure 49).

Data from a borehole temperature log show a different trend (Figure 48). The data indicate no significant geothermal gradient. The data all remain near the annual average temperature of 17 C (62.5°F) (Fairchild et al, 1990). Water sample data collected from various sources indicate a similar trend. Data from Christenson et al. (2009) found only 5 temperatures for springs or wells above 20 C (68°F), out of 36 samples collected. Four of the samples were between 20 C and 22.5 C, but three of these samples were sampled from Spears 2 well at the surface during July, and were likely heated somewhat during sampling. The only one which exceeded 25 C (77°F) (Figure 49), was a brine sample from 3890 feet deep in the Simpson. Data from Fairchild et al. (1990) found 43 samples below 20 C, 3 between 20 C and 25 C, and none above 25 C. The three wells above 20 C were located in townships 2 south, 1 and 2 east at the edge of the aquifer. Spring data for the aquifer indicate that the springs are “ambient” springs flowing at near the average annual temperature for the area.

Arbuckle-Simpson Petroleum Bottom-Hole Temperature Data					
Well location	Total Depth [Feet]	Maximum Temperature [degrees F]	Well location	Total Depth [Feet]	Maximum Temperature [degrees F]
4-1N-3E	1885	90	7-2N-3E	2527	92
11-1N-3E	1798	87	10-2N-3E	1263	85
17-1N-3E	1448	85	19-2N-3E	6300	130
30-1N-3E	1597	86	21-2N-3E	2115	95
32-1N-3E	800	86	31-2N-3E	2230	96
32-1N-3E	5186	118	5-2N-4E	4430	110
25-1N-4E	3460	116	16-2N-4E	775	80
27-1N-5E	3262	85	34-2N-4E	613	85
3-1N-7E	6210	122	12-2N-5E	4740	118
12-1N-7E	8978	131	17-1S-3E	2200	100
2-2N-3E	4923	120	22-1S-3E	2180	102
3-2N-3E	1703	90	13-2S-4E	3509	108

Table 1. Petroleum bottom-hole temperature data for the Arbuckle-Simpson aquifer (from Puckette et al., 2009).

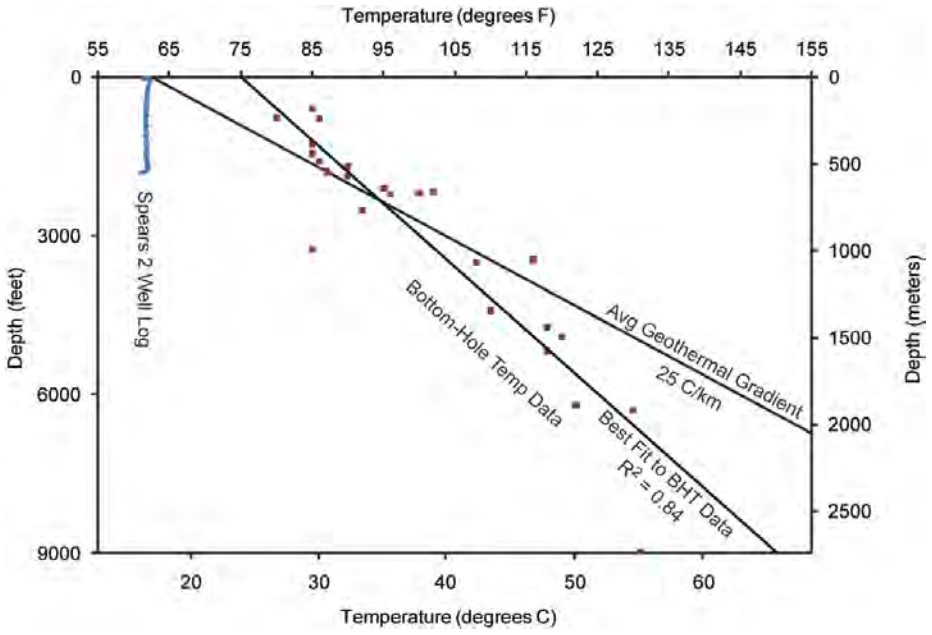

Figure 48. Temperature log from Spears 2 well and petroleum well bottom-hole temperature data compared to "normal" geothermal gradient of 25 degrees C/ kilometer.

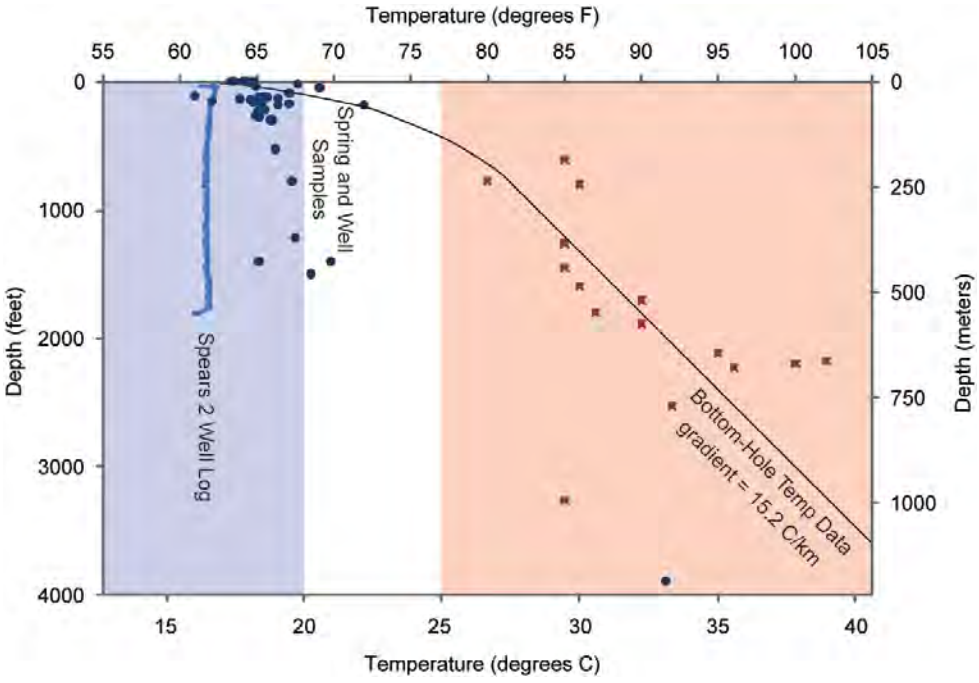

Figure 49. Temperature log from Spears 2 well compared against bottom-hole temperatures collected across the Hunton anticline region and well and spring temperature data (Puckette et al., 2009 and Christenson et al., 2009). A category of "typical" Hunton anticline temperature is denoted in blue below 20 C (68° F) and outside warmer temperatures above 25 C (77 ° F).

5.3 Discussion

The two primary issues to address for the aquifer with vertical fracture data is the amount of connection and circulation that occurs throughout the thickness of the aquifer, and the possible influence of pumping on the surface springs and streams of the aquifer. The data for the aquifer provide good evidence for understanding these two issues.

The best evidence for the vertical connection and circulation for the aquifer is from the temperature data available for the aquifer. The borehole-temperature data suggest the upwelling of fluids from depth around the edges of the aquifer that bring heat up from depth, but the well log and water sample data indicate that in the interior of the aquifer, water must be moving vertically downward rapidly. In order to cool the rocks and fluid samples 10 – 15 C below the expected temperature, and to maintain a geothermal gradient near zero, fluids must be moving up and down through the aquifer rapidly.

This data is supported by the fluid chemistry in the Spears 2 uncased well which shows no appreciable chemical gradients over a 550 meter (1800 foot) range of thickness of the aquifer. Young groundwater age dates also support this interpretation (Christensen et al., 2008). The results from this well were unexpected. In order to evaluate the data more thoroughly, vertical flow was analyzed from the logs and showed flow moving both up and down the bore at different intervals. The logging instrument was tested and reran in the bore. Packer tests were used to measure temperature from water samples at ground level, providing a similar temperature with a completely different instrument and method. As scientific drilling in the aquifer is expensive, this is the only high quality data we have for temperature at depth within the aquifer from a recently drilled borehole. The vertical flow is also supported by numerous geophysical methods suggesting dominant vertical fracturing located throughout the aquifer.

Uncertainty remains about the location of the bottom of the circulation system of the Arbuckle-Simpson aquifer. The formation thickness exceeds 1000 meters in locations (Faith et al, 2009), but the location of the bottom of vertical circulation is not fully known. Based on the vertical fracturing evident in the seismic data, and the geologic mapping of faults, it is likely that the zone of vertical circulation extends to at least the basement. At this depth of approximately 1000 meters, the best evidence for connection to the surface would be water sample

temperatures near or below 25 C (77°F) with subsequent sampling for young groundwater ages less than 50 years.

The effects of pumping at depth in the aquifer can be predicted with the data on aquifer circulation. As spring temperatures are ambient, one could assume that they were entirely shallow flow systems and may be hydraulically disconnected from waters at depth. However, the entire system is ambient with depth, therefore, the surface spring water chemistry and temperature may be fully connected with the bottom of the aquifer. It is possible that this connection is stronger than connections laterally between springs and wells. Until careful tests are performed at the bottom of the aquifer, the relative strength of these connections will remain uncertain.

6.0 Conclusions

In evaluating controls that fractures in the Arbuckle-Simpson aquifer may exert over horizontal flow, GIS data for streams and faults were evaluated in the context of hydraulic and outcrop data. The advantage of using a GIS layer of streams and faults to characterize subsurface aquifers was the amount of data available. The statistical analysis indicated a correlation between stream and fault orientations, and this correlation between the streams and faults was used to infer subsurface characteristics as demonstrated by correlation with outcrop fracture data. The polymodal orientation method used in this study was an effective way to analyze orientations and allows for consistent orientation signals to become obvious even when there was little separation between signals. The method used to study the aquifer was cost effective with limited bias in studying aquifer characteristics.

The results indicated that a dominant $170^{o} – 0^{o}$ trend (degrees from north) evident in stream data exists over the study area as well as a less dominant $20 – 30^{o}$ trend that exists in both stream and fault data. The dominant fault orientation at 115^{o} did not provide a statistically significant signal in either fault or stream data. The stream density data indicated that no trends exist between density or length and stratigraphy, but geological processes appeared to have a significant influence on stream orientations in the study area. The $170^{o} – 0^{o}$ trend appeared to exert the largest control over surface water features, and appeared to align with convergent flow patterns in most streams over the discharge region of the Hunton anticline. The obvious exception is the Blue River which appeared to be controlled by the location of the Simpson formation in the eastern portion of the Hunton anticline. The dominant fault orientation at 115° does appear to influence groundwater, at least in the northern portion of the Hunton anticline where it provided a linear connection between the orientation of the Blue River and the location of Byrds Mill Spring.

The evaluation of vertical fracturing included geophysical and thermal datasets. The results indicated that the aquifer is well connected vertically with flow processes nearly eliminating any geothermal gradient in the aquifer. The geophysical methods applied to the aquifer include seismic, gravity, and electrical methods, and all methods observed significant vertical fracturing, which available data indicated extends to the bottom of the aquifer. The lower boundary of the groundwater flow system is still poorly defined, but is likely to be 1000 meters or greater in some areas.

7.0 References

Belt, K., Paxton, S.T. (2005). “GIS as an aid to visualizing and mapping geology and rock properties in regions of subtle topography.” GSA Bulletin **117**(1/2): 149-160.

Blanchet, P. H. (1957). "Development of fracture analysis as exploration method." Bulletin of the American Association of Petroleum Geologists **41**(8): 1748-1759.

Cemen, I., Young, R., Halihan, T. (2008). “Determination of Fracture Density in the Arbuckle-Simpson Aquifer from Ground Penetrating Radar (GPR) and Resistivity Data “, OWWRI Report, 48 p.

Christenson, S., Hunt, A.G., and Parkhurst, D.L. (2009). “Geochemical investigation of the Arbuckle-Simpson aquifer, South-central Oklahoma, 2004-2006.” U.S. Geological Survey Scientific Investigations Report 2009-5036, 50 p.

Cladouhos, T.T., Marrett, R. (1996). “Are fault growth and linkage models consistent with power-law distributions of fault lengths?” Journal of Structural Geology **18**:(2/3): 281-293.

Decker, C.E, Merritt, C.A. (1931). “The stratigraphy and physical characteristics of the Simspon group.” Oklahoma Geological Survey Bulletin **55**: 5-100.

Denison, R.E., (1995). “Significance of air-photograph linears in the basement rocks of the Arbuckle Mountains.” Oklahoma Geological Survey Circular **97**: 119-131.

Dott R. (1933). “Overturned beds in the Arbuckle Mountains, Oklahoma.” Bulletin of the American Association of Petroleum Geologists **17**(7): 865-868.

Dott R. (1934). “Overthrusting in Arbuckle Mountains, Oklahoma.” Bulletin of the American Association of Petroleum Geologists **18**(5): 567-602.

Evenson, R.A. (1989). “Depositional, diagenetic, and tectonic influences on permeability and porosity in two Cherokee sandstone reservoirs, Greenwood County, Kansas.” University of Kansas Master’s thesis.

Fairchild, R. W., Hanson, R.L., Davis, R.E. (1979). "Aquifer characteristics of the Arbuckle aquifer, south-central Oklahoma." Geological Society of America (GSA) - Abstracts with Programs, South-Central Section **11**: 147.

Fairchild, R. W., Hanson, R.L., Davis, R.E. (1990). Hydrology of the Arbuckle Mountains Area, south-central Oklahoma.

Freisatz, W.B. (1991). “Fracture-enhanced porosity and permeability trends in the Bakken Formation, Williston Basin, western Dakota.” University of North Dakota Master’s thesis.

Gleeson, T., Novakowski, K. (2009). “Identifying watershed-scale barriers to groundwater flow: lineaments in the Canadian Shield”, Geological Society of America Bulletin, **121** (3-4): 333-347, DOI: 10.1130/B26241.1.

Ham, W.E. (1955). “Geology of the Arbuckle Mountain region.” Oklahoma Geological Survey Guidebook 1-61.

Ham W.E., Denison, R.E., Merritt, C.A. (1964). “Basement rocks and structural evolution of southern Oklahoma.” Oklahoma Geological Survey Bulletin **95**: 7-209.

Johnson, K.S. (1991a). “Arbuckle group core workshop and field trip.” Oklahoma Geological Survey **91-3**: 3-263.

Johnson, K.S. (1991b). “Late Cambrian-Ordovician geology of the southern mid-continent, 1989 symposium.” Oklahoma Geological Survey Circular **92**: 3-226.

Kennedy, B. (2008). “Seismic features of the Arbuckle-Simpson aquifer determined from surveys at three different geologic scales.” University of Oklahoma Master’s Thesis.

Lattman, L. H., Parizek, R.R. (1964). "Relationship between fracture traces and the occurrence of ground water in carbonate rocks." Journal of Hydrology **2**(2): 73-91.

Leveinen J., Ronka, E., Tikkanen, J., Karro, E. (1998). “Fractional flow dimensions and hydraulic properties of a fracture-zone aquifer, Leppävirta, Finland.” Hydrogeology Journal **6**: 327-340.

Mabee, S. B., Curry, Patrick J., Hardcastle, Kenneth C. (2002). "Correlation of lineaments to ground water inflows in a bedrock tunnel." Ground Water **40**(1): 37-43.

Mabee, S. B., Hardcastle, K. C. (1997). "Analyzing outcrop-scale fracture features to supplement investigations of bedrock aquifers." Hydrogeology Journal **5**(4): 21-36.

Magowe, M. (1999). "Relationship between lineaments and ground water occurrences in western Botswana." Ground Water **37**(2): 282-286.

Marrett, R. (1996). “Aggregate properties of fracture populations.” Journal of Structural Geology **18**(2/3): 169-178.

Marrett, R., Ortega, O.J., Kelsey, C.M. (1999). “Extent of power-law scaling for natural fractures in rock.” Geology **27**(9): 799-802.

Marshak, S., Nelson, W.J., McBride, J.H. (2003). “Phanerozoic strike-slip faulting in the continental interior platform of the United States: examples from the Laramide Orogen, Midcontinent, and Ancestral Rocky Mountains.” The Geological Society of London **210**: 159:184.

McQuillan, H. (1986). “The role of basement fracturing in oil production from the oil fields of the Zagros fold belt in southwest Iran.” Fifth international conference on basement tectonics. Cairo, Egypt. Oct. 16-18.

Mollard, J. D. (1957). "Aerial photographs aid petroleum search." Candian Oil and Gas Industries **10**(7): 89-96.

Moore, R. B., Schwarz, Gregory E., Clark, Stewart F. Jr., Walsh, Gregory J., Degnan, James R. (2002). "Factors related to well yield in the fractured-bedrock aquifer of New Hampshire." USGS.

Mouri, S. (2006). “Using streams and faults as lineaments to delineate aquifer characteristics” Oklahoma State University, Master’s Thesis, 62 pp plus appendices.

Or, D., Tuller, M. (2000). “Flow in unsaturated fractured porous media: hydraulic conductivity of rough surfaces.” Water Resources Research **36**(5): 1165-1177.

Ortega, O.J., Marrett, R.A., Laubach, S.E. (2006). “A scale-independent approach to fracture intensity and average spacing measurement.” AAPG Bulletin **90**(2): 193-208.

Parizek, R. R. (1975). On the nature and significance of fracture traces and lineaments in carbonate and other terranes. Proc. of the U.S. Yugoslovian Symposium.

Puckette, J., Halihan, T., Faith, J. (2009). “Characterization of the Arbuckle-Simpson aquifer”. Report to the Oklahoma Water Resources Board, 56 pp plus appendices.

Rahi, K., Halihan, T. (2009) “Estimating Selected Hydraulic Parameters of the Arbuckle-Simpson Aquifer from the Analysis of Naturally-Induced Stresses.” Report to the Oklahoma Water Resources Board, 50 pp plus appendix.

Rumsey, I. A. P. (1971). "Relationship of fractures in unconsolidated superficial deposits to those in the underlying bedrock." Modern Geology **3**: 25-41.

Sander, P., Minor, Timothy B., Chesley, Matthew M. (1997). "Ground-water exploration based on lineament analysis and reproducibility tests" Ground Water **35**(5): 888-894.

Scheirer, D. S. and A. H. Scheirer (2006). Gravity Investigations of the Chickasaw National Recreation Area, south-central Oklahoma, USGS**:** 42.

Smith, B.D., Blome, C.D., Smith, D.V., Scheirer, D.D., Deszcz-Pan, M., Halihan, T. (2008), “Geophysical Surveys to Characterize the Hydrogeology of the Arbuckle Uplift, South-Central Oklahoma, 21st SAGEEP, Symposium on the Application of Geophysics to Engineering and Environmental Problems, Philadelphia, PA.

Terech, N. (2005). “Fracture patterns, lineaments and seismic reflection data; integration for fault mapping in the Appalachian Basin of east-central New York State.” Geological Society of America (GSA) - Abstracts with Programs **37**(1): 83-84.

Wanfang, Z., Wheater, H.S., Johnston, P.M. (1997). “State of the art of modelling two-phase flow in fractured rock.” Environmental Geology **31**(3/4): 157-166.

Wickham, J. (1978). “The southern Oklahoma aulacogen.” Geological Society of America-South Central Section 9-41.

Zimmerman, R.W., Bodvarsson, G.S. (1996). “Hydraulic conductivity of rock fractures.” Transport in Porous Media **23**: 1-30.